

The O-Ti (Oxygen-Titanium) System

15.9994

47.88

By J.L. Murray*
National Bureau of Standards

and

H.A. Wriedt
Consultant

Introduction

This assessment of the Ti-O system covers the phase equilibria and crystal structures of the condensed phases in the composition range between pure Ti and TiO_2 . The thermodynamic properties of the Ti oxides have been studied and assessed extensively [75Cha]. The present assessment does not duplicate [75Cha]; coverage of thermochemical properties is limited to recent work. So far as possible, melting points and solid-state transition temperatures in the present diagram agree with [75Cha], so that the two assessments may be used together.

The assessed Ti-O phase diagram is shown in Fig. 1, and its important features have been summarized in Table 1. The temperature range in which a reasonable equilibrium diagram can be constructed excludes some phase transitions of the higher oxides, and it has not been possible to

include all of the observed higher oxide phases in a diagram. However, Tables 1, 2, and 3 contain complete listings of the phases and phase transitions.

O has a large solubility in low-temperature cph (αTi), and it stabilizes (αTi) with respect to the high-temperature bcc form, (βTi). At low temperature, the ordered cph phases Ti_2O , Ti_3O , and, possibly, Ti_6O are formed with some homogeneity range.

Structures of the monoxides are based on the NaCl structure of the high-temperature γTiO form. Four additional structural modifications were identified, which here are designated βTiO , αTiO , $\beta\text{Ti}_{1-x}\text{O}$, and $\alpha\text{Ti}_{1-x}\text{O}$. In this assessment, "TiO" refers to the monoxides without restriction to a particular variety. The phase boundaries separating these phases, except for the disordering of αTiO , were not determined; the phase boundaries of the monoxides in equilibrium with (αTi) and with $\beta\text{Ti}_2\text{O}_3$ were determined, but without distinguishing the various monoxide modifications.

The stable condensed phase richest in O is rutile (TiO_2). In addition to rutile, TiO_2 has two nonequilibrium low-pres-

* Present address: Alcoa Technical Center, Alloy Technology Division, Alcoa Center, PA 15069.

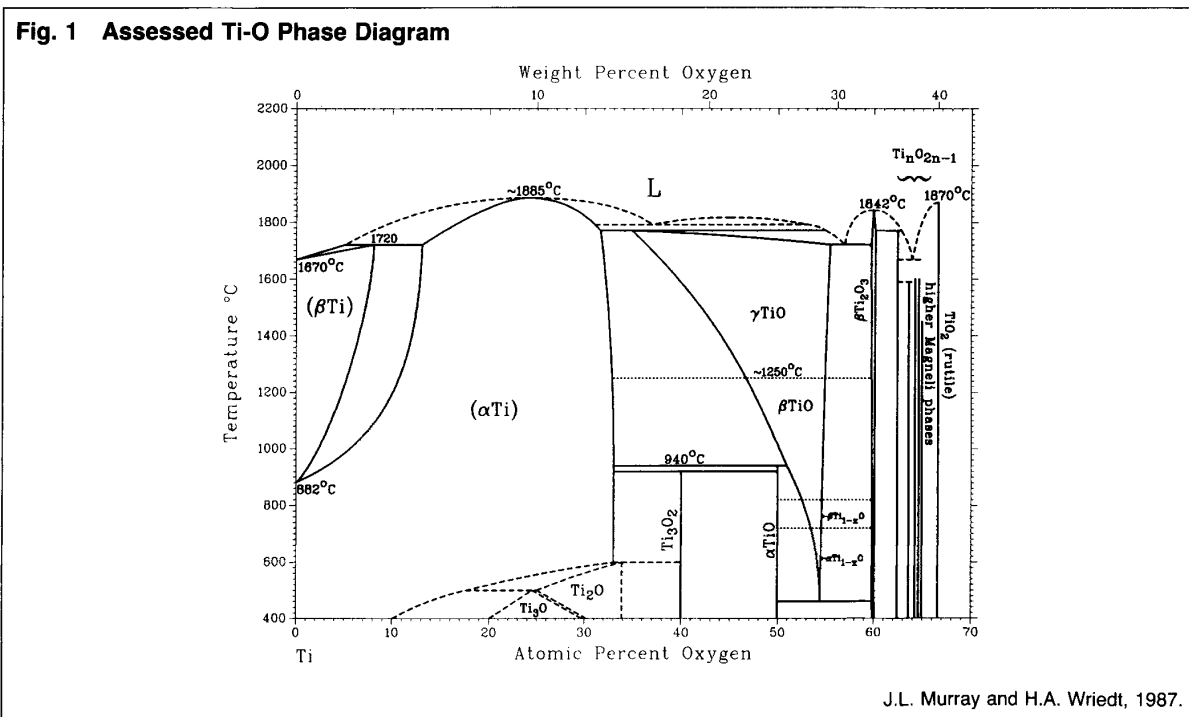


Table 1 Special Points of the Assessed Ti-O Phase Diagram

Reaction	Compositions of the respective phases, at.% O			Temperature, °C	Reaction type
L + (α Ti) \rightleftharpoons (β Ti)	5	13	8	1720 \pm 25	Peritectic
L \rightleftharpoons (α Ti)		~24		1885 \pm 25	Congruent point
(α Ti) + Ti ₃ O ₂ \rightleftharpoons Ti ₂ O	33.3	40	33.9	~600	Peritectoid
(α Ti) + Ti ₂ O \rightleftharpoons Ti ₃ O	~17	~25	~24.5	~500	Peritectoid
L \rightleftharpoons (α Ti) + L	~37	~31	~53	~1800	Monotectic?
L + (α Ti) \rightleftharpoons γ TiO	~55	31.4	34.5	1770	Peritectic
γ TiO \rightleftharpoons β TiO		~1250	Unknown
β TiO \rightleftharpoons β Ti _{1-x} O	Unknown
β Ti _{1-x} O \rightleftharpoons α Ti _{1-x} O	Unknown
(α Ti) + β TiO \rightleftharpoons α TiO	33.3	51	50	940	Peritectoid
(α Ti) + α TiO \rightleftharpoons Ti ₃ O ₂	32.4	50	40	920	Peritectoid
α Ti _{1-x} O \rightleftharpoons α TiO + β Ti ₂ O ₃	54.5	50	60	460	Eutectoid
L \rightleftharpoons γ TiO + β Ti ₂ O ₃	~57	54.5	59.8	1720	Eutectic
L \rightleftharpoons β Ti ₂ O ₃		60		1842	Congruent point
L + β Ti ₂ O ₃ \rightleftharpoons β Ti ₃ O ₅	63	60.2	62.5	1770	Peritectic
β Ti ₂ O ₃ \rightleftharpoons α Ti ₂ O ₃		60		~180	Unknown
β Ti ₃ O ₅ \rightleftharpoons α Ti ₃ O ₅		62.5		187	Unknown
γ Ti ₄ O ₇ \rightleftharpoons β Ti ₄ O ₇		63.64		-123	Unknown
β Ti ₄ O ₇ \rightleftharpoons α Ti ₄ O ₇		63.64		-148	Unknown
L \rightleftharpoons β Ti ₃ O ₅ + ?	~64	62.5	...	~1670	Eutectic
β Ti ₃ O ₅ + β Ti ₅ O ₉ \rightleftharpoons γ Ti ₄ O ₇	62.5	64.29	63.64	~1500	Peritectoid
L \rightleftharpoons TiO ₂		66.7		1870	Congruent point
L \rightleftharpoons (β Ti)		0		1670	Melting point
(β Ti) \rightleftharpoons (α Ti)		0		882	Allotropic transformation

sure forms (anatase and brookite) and two nonequilibrium high-pressure forms (TiO₂-II and TiO₂-III).

Between the monoxides and TiO₂ is a series of discrete phases with stoichiometry Ti_nO_{2n-1}, where $n \geq 2$, which are called Magneli phases. It was suggested that discrete equilibrium phases exist for $n \leq 99$ [72Roy]. Ti_nO_{2n-1} ($4 \leq n \leq 10$) phases have crystal structures derived from the rutile structure by crystallographic shear. Closely related structures were observed and described as coherent intergrowths of Magneli phases [70And] or as families of phases based on different crystallographic shear operations [69Bur, 71Bur1, 71Bur2]. Magneli phases undergo one or more structural, electrical, or magnetic transitions at low temperature.

Equilibrium Diagram

Terminal Solid Solutions and Suboxides

(α Ti) + (β Ti) Phase Field. Experimental data on the (α Ti)/(β Ti) equilibria are compared with the assessed diagram in Fig. 2. The following experimental techniques were used:

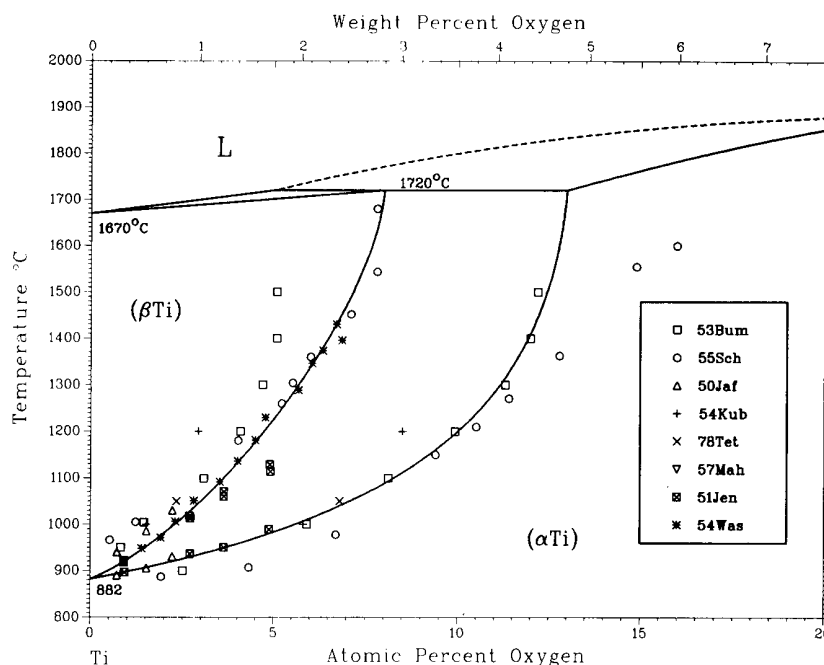
- Metallography [50Jaf, 53Bum, 56Sch]
- Thermoelectric power measurements and metallography [51Jen]
- Thermodynamic measurements [54Kub, 57Mah, 78Tet]
- Analysis of diffusion specimens [54Was]

[51Jen] showed that the impurities present in commercial-grade Ti were sufficient to cause a marked (>1 at.%) broadening of the (α Ti) + (β Ti) field. Thermoelectric power data [51Jen] for high-purity alloys showed well defined discontinuities in slope for the (α Ti) transus, but were difficult to interpret for the (β Ti) transus above 1050 °C.

Table 2 Experimental Congruent and Incongruent Melting Temperatures

Phase	Reference	Temperature °C	Comment
γ TiO	[37Daw]	1750	Incongruent
	[54Dev]	1830	
	[56Nis]	1750	
β Ti ₂ O ₃	[75Cha]	1750	Congruent
	[54Dev]	1920	
	[56Sch]	1800	
	[56Nis]	1830	
	[60Bra]	1820 \pm 15	
	[66Wah, 67Gil]	1842 \pm 10	
β Ti ₃ O ₅	[73Sly]	1770	Incongruent
	[75Cha]	1842	
	[66Wah, 67Gil]	1774 \pm 10	
	[54Dev]	1900	
	[73Sly]	1810	
γ Ti ₄ O ₇	[75Cha]	1777	Probably incongruent
	[71Ham]	<1670	
	[73Sly]	1720	
	[75Cha]	1677 \pm 20	
Rutile	[73Sly]	1741	Congruent
	[60Bra]	1870	
	[54Dev]	1830 \pm 10	
	[56Nis]	1825	
	[75Cha]	1870	

For the (β Ti) transus, the data of [56Sch] are preferred, because they were corroborated by the diffusion experiments of [54Was]. The data of [51Jen] are preferred for the low-temperature part of the (α Ti) transus. For the (α Ti) transus above 1300 °C, where the data of [53Bum] and [56Sch] were scattered and disagreed with each other by as much as 2 at.%, there is no clear basis for preferring the data of either. In constructing the assessed transus, the liquidus and solidus have been considered. The (α Ti) boundaries must be drawn so that the liquidus and solidus

Fig. 2 Experimental Data for the (α Ti)/(β Ti) Phase Boundaries


J.L. Murray and H.A. Wriedt, 1987.

can be extrapolated to a metastable melting point of pure cph Ti. The roughly extrapolated melting point falls at about 1425 °C, in good agreement with the theoretical prediction of [70Kau].

Ti-Rich Liquidus and Solidus. Optical pyrometry was used by [53Bum] and [56Sch] to determine the temperature of the peritectic reaction $L + (\alpha\text{Ti}) \rightleftharpoons (\beta\text{Ti})$. [53Bum] found 1740 ± 25 °C (relative to 1720 °C for "pure" Ti); [56Sch] found 1720 ± 25 °C (relative to 1660 °C for "pure" Ti). The value 1720 ± 25 °C is used in this evaluation.

(α Ti) with 24 at.% O melts congruently at 1885 ± 25 °C, according to optical pyrometric melting point data [53Bum, 56Sch, 65Kor] (Fig. 3). The schematic (α Ti) liquidus (Fig. 1), is based on the endpoint compositions at the invariant reactions. Experimental liquidus data for the whole system are shown in Fig. 3.

(α Ti) Homogeneity Range. [53Bum], [56Sch], and [70Jos] examined the (α Ti)/(α Ti) + TiO boundary from 600 °C to the melting point, using X-ray diffraction (XRD) and metallography on quenched specimens. Additional data were provided over limited temperature ranges by [60Mak] (lattice parameter); [59Yao] and [63Vas] (magnetic susceptibility); [66Dub] (hardness); [76Bou] and [78Tet] (partial Gibbs energy); and [57Kon], [63Kor], [71Dub1], [71Dub2], and [71Dub3] (microstructure and lattice parameter). Selected experimental data are shown in Fig. 4.

Below 1000 °C, there is a discrepancy between the vertical phase boundary reported by [53Bum] and the decreasing O solubility at lower temperature reported by [56Sch]. The magnetic susceptibility results of [59Yao] agreed with those of [56Sch] but are not sufficiently accurate to be con-

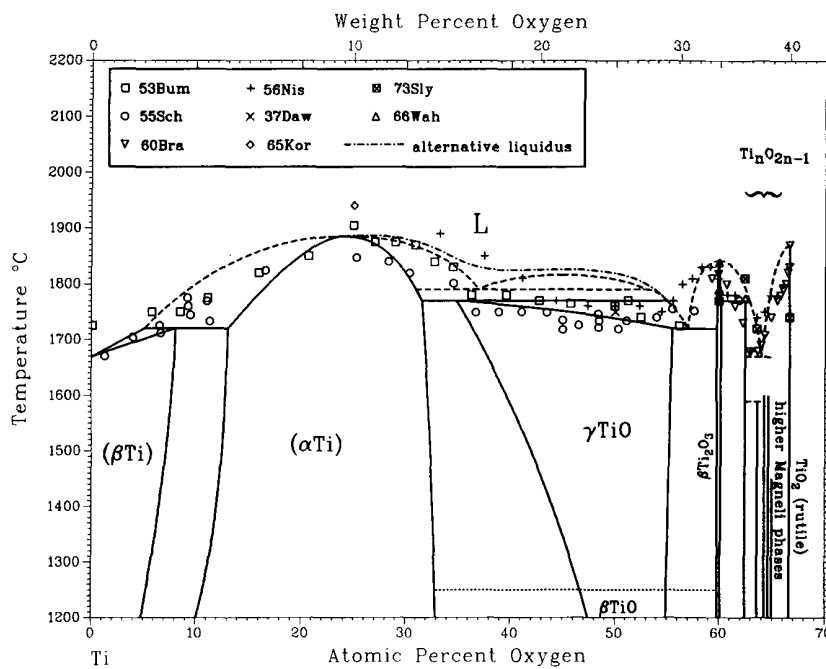
sidered definitive. [70Jos] suggested that [56Sch] may have misinterpreted banded microstructures associated with etching effects on faulted (α Ti) alloys as evidence for TiO precipitation. The work of [53Bum] is supported by lattice parameter data [70Jos] and further metallographic work [57Kon, 63Kor]; therefore, it has been used in the present assessment.

Above 1400 °C, the assessed diagram is based on [70Jos], who showed that single-phase (α Ti) alloys transformed on heating to (α Ti) + TiO structures. [70Jos] placed the solubility of O in (α Ti) between 30.9 and 31.6 at.% O at the $L + (\alpha\text{Ti}) + \gamma\text{TiO} + L$ peritectic temperature.

Ordered Hexagonal Phases (Suboxides). Several qualitatively different pictures were given for the phase equilibria involving the ordered hexagonal phases. Ti_2O (also designated α' [70Jos, 69Yam] or $\text{Ti}_2\text{O}_{1-y}$ [57And1, 62Hol]) and Ti_3O are well established phases. Ti_6O [63Kor, 70Kor, 79Dav] and Ti_{12}O also were proposed as equilibrium phases. However, a single-ordered phase with compositions ranging from near Ti_2O to quite low O content may encompass the phases distinguished previously as Ti_3O and Ti_6O , and possibly Ti_{12}O , as well. In the present assessment, this phase has been designated Ti_3O to avoid proliferation of nomenclature.

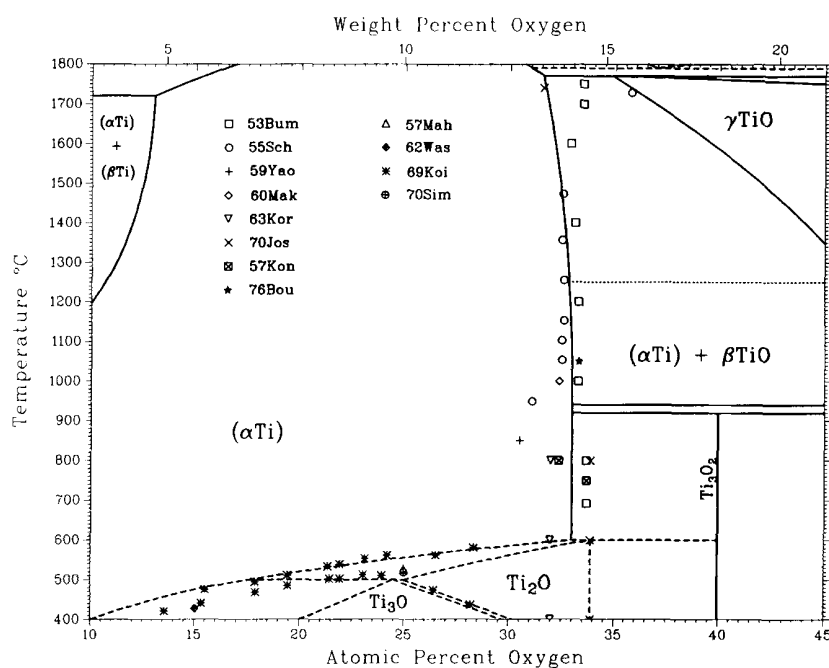
In all of the ordered hexagonal phases, O resides in octahedral sites in layers alternating with Ti. Ti_2O has the anti- CdI_2 structure (space group $P3m1$) with alternate O layers vacant, and additional vacancies distributed randomly in the occupied layer [57And1, 59Now, 62Hol, 69Yam, 70Yam, 62Hol, 71Dub1, 71Dub2, 71Dub3]. For alloys containing up to 33.3 at.% O (at which all sites in the plane are occupied) ordering can occur within the occupied

Fig. 3 Experimental Liquidus Data for the Ti-O System



J.L. Murray and H.A. Wriedt, 1987.

Fig. 4 Experimental Data for Phase Boundaries Involving the Hexagonal Phase



J.L. Murray and H.A. Wriedt, 1987.

plane, lowering the symmetry to $P\bar{3}1c$ [62Hol, 69Yam, 70Kor, 70Yam, 71Dub1, 71Dub2, 71Dub3]. Three equivalent sites are available in the plane, which are filled successively at Ti_6O , Ti_3O and Ti_2O .

Thus, the special compositions Ti_5O and Ti_3O may have distinct structures; alternatively, they may belong to a single phase in which the sites are filled successively but in completely continuous fashion. $P\bar{3}m1$ is a halving subgroup of $P6_3/mmc$ (of the completely disordered phase); therefore, a second-order transition, $(\alpha Ti) \rightleftharpoons Ti_2O$, is not ruled out by symmetry considerations. $P\bar{3}1c$, however, is not a halving subgroup of $P\bar{3}m1$; consequently, a second-order transition is ruled out for the $Ti_2O \rightleftharpoons Ti_3O$ transition, by the Landau criterion.

Ti_2O was discovered by [57And1], [57And2], [59Now], and [60Mak]. Single-phase Ti_2O was found within the range 22.5 to 33.3 at.% O in as-solidified alloys [71Dub1]. [62Hol] found Ti_2O in stoichiometric alloys quenched from 1800 °C; in other alloys, it was found only after low-temperature annealing. Ti_3O was found only in 25 at.% O alloys heat treated at 400 °C. These results were verified in all of their qualitative features by [66Dub], [68Mod], and [70Jos].

Based primarily on physical and mechanical properties of quenched alloys, it was proposed that Ti_2O [57And1, 62Hol, 68Mod] or Ti_3O [63Kor, 65Kor, 66Dub] is stable to the melt. [70Jos] presented indirect microstructural evidence that Ti_2O forms in the solid state. Work at temperature [57Mah, 62Was, 66Yam, 69Hir, 69Koi, 70Sim2, 70Yam] showed that both Ti_2O and Ti_3O are formed only below about 600 °C. Observations of the ordering reactions by resistivity [62Was], heat capacity [56Mah, 69Koi], and structural analysis [70Sim1, 70Sim2, 70Yam] are in good agreement, as shown in Fig. 4. Two-phase structures were not found by optical microscopy [68Mod]. This area of the assessed diagram is a tentative, schematic construction based on the data shown in Fig. 4.

From C_p -vs-temperature and order parameter-vs-temperature measurements, [69Koi] and [69Hir] proposed that both ordering reactions, $(\alpha Ti) \rightleftharpoons Ti_2O \rightleftharpoons Ti_3O$, proceed as second-order phase transitions. As pointed out above, this assertion for the second reaction is ruled out by the Landau criterion. The present authors believe that the heat capacity data of [69Koi] are interpreted most plausibly as evidence for a three-phase reaction of (αTi) , Ti_2O , and Ti_3O , as shown schematically in the assessed diagram.

The diagram proposed by [63Kor], [65Kor], [70Kor], and [73Kor] differed from all others. Ti_6O was shown as stable to 820 °C with a wide two-phase $Ti_6O + (\alpha Ti)$ field. Ti_3O was shown as a line compound in the single-phase (αTi) field (sic) and stable to the melt. Ti_2O was not shown. None of these features was verified; consequently, this diagram has not been considered further. Ti_6O was also thought to be a distinct phase by [66Yam], [71Dub1], [71Dub2], [71Dub3], and [79Dav]. Because concrete evidence for a phase transition between Ti_3O and Ti_6O was lacking, and also from structural considerations, the present authors do not consider Ti_6O to be a distinct phase.

In summary, the ordered cph phases were shown in various compilations either as discrete compounds or as

phases of wide homogeneity range produced from the disordered phase by second-order transitions. They were shown as persisting to the melting point, or as disordering above about 600 °C. According to crystal structure data, ordering on the O sublattice occurs over a wide composition range, and it is erroneous to show these phases as discrete compounds. Evidence for the persistence of the ordered phases to the melting point was indirect; direct observations of disordering at lower temperatures have been preferred as the basis for the assessed diagram. Detailed placement of phase boundaries, however, is still very uncertain.

Ti_3O_2 (usually designated δ in the experimental literature) was observed [53Bum, 56Sch, 57Kon] to occur only below 800 to 900 °C. Originally, the crystal structure was thought incorrectly to be tetragonal. Ti_3O_2 was not obtained as a single phase [57And1, 59And]. Microstructures of alloys containing Ti_3O_2 are not typically peritectoid, but the conditions of temperature and composition range in which Ti_3O_2 forms suggested that it is produced by the reaction $(\alpha Ti) + \alpha TiO \rightleftharpoons Ti_3O_2$ [53Bum, 56Sch, 57And1, 57Kon, 59And]. The crystal structure was determined by [59And] to be hexagonal, an ordered structure with ideal stoichiometry Ti_3O_2 . In the assessed diagram, the peritectoid reaction has been set at 920 °C, on the basis of the values 925 and 910 °C of [53Bum] and [56Sch], respectively. The location of the composition at 40 at.% O is from [57And1] and [57Kon].

The Monoxides

Liquidus and Solidus. Over the composition region 34.5 to 55.6 at.% O, the homogeneity range of γTiO , alloys begin to melt in the narrow range of 1770 to 1720 °C. These data were interpreted previously in three ways:

- The reaction of L, γTiO , and Ti_2O_3 is peritectic. This implies that γTiO melts congruently with a minimum melting point [56Nis, 70Jos, Elliott].
- The reaction of L, γTiO , and Ti_2O_3 is eutectic and occurs at a temperature below 1770 °C. The melting of γTiO is then incongruent. If the peritectic composition for the reaction $L + (\alpha Ti) \rightleftharpoons \gamma TiO$ is placed near 35 at.% O, then the two-phase L + γTiO field is a narrow lens [53Bum, 66Wah].
- The reaction of L, γTiO , and Ti_2O_3 is eutectic and it occurs below 1770 °C; γTiO melts incongruently, as above. However, if the peritectic composition is placed nearer 55 at.%, both the L + (αTi) and L + γTiO two-phase fields broaden as much as 20 at.% over a narrow (~50 °C) temperature interval, as the peritectic temperature is approached from above and below (see Fig. 3).

These constructions are very unusual and require care to draw a diagram consistent with the rules of phase diagram construction. In this assessment, the observed melting points have been interpreted in terms of a liquid miscibility gap (see Fig. 3).

In addition to the determinations of incipient melting temperatures shown in Fig. 3 and Table 2, two observations were reported about the melting in this region:

- By metallographic examination of alloys quenched from temperatures near the melting point, [56Sch] found evidence for $(\alpha Ti) + L$ and $\gamma TiO + L$ phase fields over a wide composition range, but a small temperature range.

- [51Jen], in a discussion of [53Bum], noted that there appeared to be a pronounced "immiscibility in the liquid melts between TiO and the higher oxides." [53Bum] corroborated the gravity segregation during preparation of compositions between TiO and TiO₂.

Based on these data, a liquid miscibility gap is shown in Fig. 1. Other investigators who prepared monoxides by arc melting did not mention such segregation [e.g., 64Den, 72Hull], and it is possible that in the binary system, the miscibility gap is metastable. Therefore, the critical temperature has been placed close to the monotectic temperature. If the miscibility gap were metastable, the liquidus would assume approximately the shape proposed by [56Sch]. The two possible liquidus curves are compared in Fig. 3.

The presence of a liquid miscibility gap, as shown in Fig. 1, would explain the sudden broadening of the L + (α Ti) phase field, whether the gap appears in equilibrium or is metastable. The miscibility gap as drawn in the present diagram is entirely qualitative.

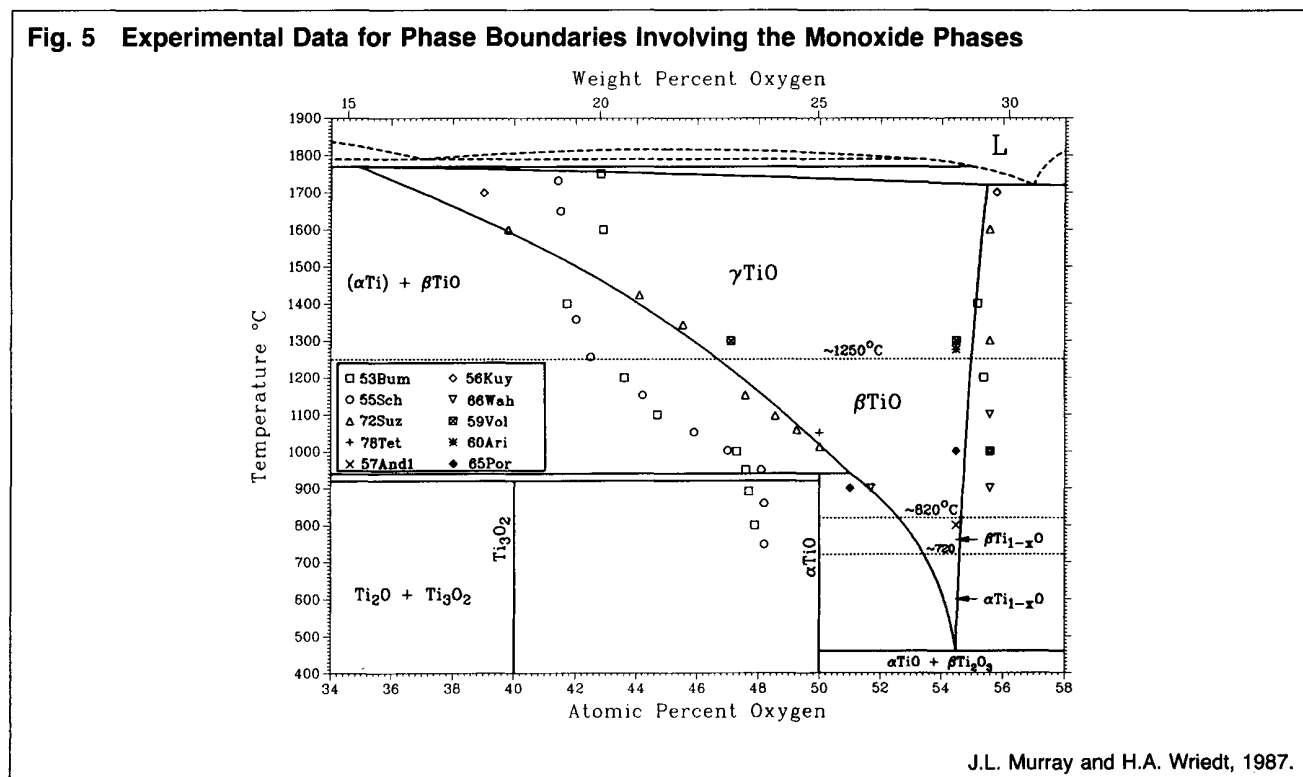
High- and Low-Temperature Monoxides. Five structural modifications of the monoxide were reported:

- γ TiO, the high-temperature form, has the NaCl structure and a wide homogeneity range. The γ TiO phase was recognized by [39Ehr] and since then has been established firmly as an equilibrium phase.
- β TiO, a cubic superstructure of ideal stoichiometry TiO, was observed by [68Hil1] in alloys heat treated below 1250 °C.
- α TiO has a narrow homogeneity range about the equiatomic composition and a monoclinic structure involving

vacancy ordering [67Wat, 68Hil2]. It was established as an equilibrium phase by a variety of experimental techniques.

- β Ti_{1-x}O has an orthorhombic structure related to that of α TiO, also based on vacancy ordering. [65Wat] and [67Wat] identified it as a metastable transition phase formed to the Ti-side of stoichiometry; [68Hil1], on the other hand, identified it as an intermediate-temperature phase (720 to 820 °C) formed in O-rich alloys (~54.5 at.% O). According to [69Ver], the same basic characteristics were found in the diffraction patterns of alloys in the entire 41.2 to 54.5 at.% O range.
- α Ti_{1-x}O has a bct structure and is the low-temperature form at O-rich compositions (~55.6 at.% O) [68Hil1, 68Wat]. The high-O monoxide structures also were designated Ti₄O₅ [68Hil1], TiO_{1.2} [60Ari], or γ' [70Jos].

Originally, only a single, NaCl-type monoxide with a wide homogeneity range was identified [39Ehr, 53Bum]. The first evidence for the low-temperature stoichiometric phase α TiO was found by [56Sch], [56Kuy], and [56Wan]; the two-phase field between α TiO and the high-temperature form was determined primarily by [65Por], [66Wah], [72Roy], and [72Suz]. However, these investigations did not take into account the other structural modifications. There is no definitive basis for judging which modifications are equilibrium binary bulk phases or where the phase boundaries and invariant reactions should be placed. The assessed diagram indicates by dotted horizontal lines the temperature ranges in which the phases were observed to form [68Hil1]; these lines do not represent quantitative phase boundaries. The following discussion of the boundaries involving (α Ti), β Ti₂O₃, or α TiO refers simply to the "high-temperature monoxide".



O-Ti

In the assessed diagram, αTiO is shown to form from the high-temperature phase by a peritectoid reaction at 940 °C. According to [53Bum], [56Sch], and [70Jos], the homogeneity range of the high-temperature form extends to about 48 at.% O down to 700 °C, and αTiO forms by a congruent transformation. The peritectoid construction of Fig. 1 is based on O activity measurements [72Suz, 78Tet] and on XRD and metallography [65Por, 66Wahj, 72Roy]. It is consistent with additional data of [56Kuy], [57And1], [59Vol], and [60Ari] as shown in Fig. 5. The peritectoid construction is based on the observation by [66Wah] that a 48.7 at.% O alloy equilibrated at 1000°C was two phase; the alloy would have been expected to be single phase for a congruent transformation anywhere below 1000 °C. The γTiO field extends to 34.9 at.% O at the peritectic temperature, according to [70Jos]. This conclusion is consistent with the data of [72Suz] in the range 1000 to 1600 °C.

There is good agreement on the temperature of the (αTi) + $\beta\text{TiO} \rightleftharpoons \alpha\text{TiO}$ peritectoid reaction. Metallography as well

as X-ray and electron diffraction placed the peritectoid reaction between 900 and 950 °C [56Wan, 57And1, 58Pea, 66Wah, 67Wat]. The assessed value of 940 °C is based on DTA [65Por, 72Roy]; the thermal analysis (heating) of [56Sch] can also be reinterpreted to give a peritectoid temperature of about 945 °C. A transformation temperature of 990 °C, based on heat content [46Nay] is too high. The narrow homogeneity range of αTiO shown in the present diagram is based on metallographic work [65Por, 66Wah]. [70Jos] proposed a somewhat larger homogeneity range (48 to 50 at.% O).

Location of the eutectoid reaction $\alpha\text{Ti}_{1-x}\text{O} \rightleftharpoons \alpha\text{TiO} + \beta\text{Ti}_2\text{O}_3$ at 460 °C is based on thermal analysis and microscopy [65Por, 72Roy].

Experimental data on the O-rich limit of the monoxide phases, obtained by XRD and metallography, located this boundary between 54.5 and 55.5 at.% O [53Bum, 56Kuy, 57And1, 59Vol, 60Ari, 65Por, 66Wah, 70Jos, 72Roy]. Ex-

Table 3 Low-Temperature Transitions of the Higher Oxides

Transition	Temperature, K	Experimental technique/comment	Reference
$\beta\text{Ti}_2\text{O}_3 \rightarrow \alpha\text{Ti}_2\text{O}_3$	473 ± 20	Heat content	[46Nay]
	453	Heat capacity	[73Bar]
	433 to 473	Lattice parameters	[58Pea]
	390 to 450	Lattice parameters	[68Rao]
	660 ± 30	Neel temperature (neutron diffraction, electrical resistivity)	[63Abr]
	~450	Magnetic susceptibility	[67Key1]
$\beta\text{Ti}_3\text{O}_5 \rightarrow \alpha\text{Ti}_3\text{O}_5$	460	Metallic → semiconductor	[69Bar]
	462	(Heating) magnetic susceptibility	[70Mul, 72Dan]
	432	(Cooling)	
	450	Heat content	[46Nay]
	373 to 393	XRD (corrected by [71Asb])	[59Asb, 61Mag]
	460		[71Asb]
	448	DTA, XRD, electrical conductivity	[71Rao]
450	Magnetic susceptibility	[65Por]	
$\alpha'\text{Ti}_3\text{O}_5 \rightarrow \alpha\text{Ti}_3\text{O}_5$	250	Metastable transformation	[71Asb]
$\gamma\text{Ti}_4\text{O}_7 \rightarrow \beta\text{Ti}_4\text{O}_7$	149 ± 2	Metallic → semiconductor	[69Bar]
	150	Metallic → semiconductor	[70Mul, 72Dan]
$\beta\text{Ti}_4\text{O}_7 \rightarrow \alpha\text{Ti}_4\text{O}_7$	150	Discontinuity in lattice parameters	[70Mar]
	125	Structural transition	[70Mul]
	125	8 to 10 K hysteresis	[69Bar]
$\gamma\text{Ti}_5\text{O}_9 \rightarrow \beta\text{Ti}_5\text{O}_9$	130	Magnetic susceptibility	[69Bar, 70Dan]
$\beta\text{Ti}_5\text{O}_9 \rightarrow \alpha\text{Ti}_5\text{O}_9$	125	Magnetic susceptibility	[69Bar]
$\beta\text{Ti}_6\text{O}_{11} \rightarrow \alpha\text{Ti}_6\text{O}_{11}$	130	Electrical conductivity	[69Bar]
	122	(DTA places transition lower)	
Ti_7O_{13} through $\text{Ti}_{10}\text{O}_{19}$	~150	Magnetic susceptibility	[70Mul, 67Key1, 67Key2]

Table 4 Homogeneity Range of Rutile (TiO_x to TiO_2)

Reference	Atomic ratio of TiO_x , x	Temperature, °C	Experimental method
[39Ehr]	~1.9	...	Thermogravimetry
[57Bra]	~1.969	~1800	...
[61Str]	1.983	1400	Lattice parameters, density
[63Blu]	1.992	1100	Isopiestic, emf
[75Pic]	~1.99	1050	Partial Gibbs energy
[77Ban]	1.992	1000	Electrical conductivity
[78Koz]	1.990	850 to 950	Solid galvanic cell
[83Zad]	1.988	1300	O potentials
	1.985	1400	
	1.982	1500	

Table 5 Ti-O Crystal Structure Data

Phase	Homogeneity range, at.% O	Pearson symbol	Space group	Strukturbericht designation	Prototype	Reference
(β Ti)	0 to 8	<i>cI2</i>	<i>Im3m</i>	A2	W	[Pearson2]
(α Ti)	0 to 31.9	<i>hP2</i>	<i>P6₃/mmc</i>	A3	Mg	[Pearson2]
Ti ₃ O	~20 to ~30	<i>hP-16</i>	<i>P31c</i>	[71Dub1, 71Dub2]
Ti ₂ O	~25 to 33.4	<i>hP3</i>	<i>P3m1</i>	...	Anti-CdI ₂	[61Mag, 62Hol]
Ti ₃ O ₂	~40	<i>hP~5</i>	<i>P6/mmm</i>	[59And]
γ TiO	34.9 to 55.5	<i>cF8</i>	<i>Fm3m</i>	B1	NaCl	[Pearson2]
β TiO	...	(a)	[68Hil1]
α TiO	~50	<i>mC16</i>	<i>A2/m</i>	[67Wat]
	<i>B*/*</i>	[68Hil2]
β Ti _{1-x} O	~55.5	<i>oI12</i>	<i>I222</i>	[65Wat, 66Yam, 68Hil1]
α Ti _{1-x} O	~55.5	<i>tI18</i>	<i>I4/m</i>	[68Wat, 68Hil1]
β Ti ₂ O ₃	59.8 to 60.2	<i>hR30</i>	<i>R3c</i>	D5 ₁	α Al ₂ O ₃	[58Pea, 68Rao, 62New]
α Ti ₂ O ₃	59.8 to 60.2	<i>hR30</i>	<i>R3c</i>	D5 ₁	α Al ₂ O ₃	[57And1, 58Pea, 68Rao]
β Ti ₃ O ₅	62.5	(b)	Anosovite	[59Asb, 51Rus]
α Ti ₃ O ₅	62.5	<i>mC32</i>	<i>C2/m</i>	[57Asb, 59Asb, 61Mag]
α' Ti ₃ O ₅ (c)	...	<i>mC32</i>	<i>Cc</i>	...	V ₃ O ₅	[71Asb]
γ Ti ₄ O ₇	63.6	<i>aP44</i>	<i>P1</i>	[63And, 73Mer, 82Lep1]
β Ti ₄ O ₇	63.6	<i>aP44</i>	<i>P1</i>	[73Mer, 84Lep]
α Ti ₄ O ₇	63.6	<i>aP44</i>	<i>P1</i>	[73Mer, 63And, 84Lep]
γ Ti ₅ O ₉	64.3	<i>aP28</i>	<i>P1</i>	[60And, 77Mar]
β Ti ₆ O ₁₁	64.7	<i>aC68</i>	<i>A1</i>	[63And, 82Lep1]
Ti ₇ O ₁₃	65.0	<i>aP40</i>	<i>P1</i>	[63And, 82Lep1]
Ti ₈ O ₁₅	65.2	<i>aC92</i>	<i>A1</i>	[63And, 82Lep1]
Ti ₉ O ₁₇	65.4	<i>aI52</i>	<i>P1</i>	[63And, 82Lep1]
Anatase(c)	...	<i>tI12</i>	<i>I4₁/amd</i>	C5	Anatase	[57And1, 55Cro]
Rutile	~66.7	<i>tP6</i>	<i>P4₂/mnm</i>	C4	Rutile	[56Bau, 57And1, 55Cro, 61Str]
Brookite(c)	...	<i>oP24</i>	<i>Pbca</i>	C21	Brookite	[59Wey, 61Yog]
TiO ₂ -II(d)	...	<i>oP12</i>	<i>Pbcn</i>	...	α PbO ₂	[66Ben, 67Sim, 67Mcq]
TiO ₂ -III(d)	...	~ <i>hP48</i>	(e)	[78Liu]

(a) Cubic. (b) Monoclinic. (c) Metastable phase. (d) High-pressure phase. (e) Hexagonal.

perimental uncertainty is sufficient to explain the spread; consequently, the assessed phase boundary is drawn between 54.5 at.% O at low temperature and 55.5 at.% O at the eutectic temperature.

[60Bri] proposed that some phase separation occurs within the γ TiO phase field, because single-phase specimens could be prepared away from stoichiometry, but 50 at.% alloys were found to be disproportionate. An explanation does not suggest itself at present.

Higher Oxides

Liquidus and Solidus. β Ti₂O₃ and TiO₂ (rutile) melt congruently. The melting points are 1842 °C [66Wah] and 1870 ± 15 °C [60Bra], respectively. [60Bra] showed that the observed melting point of rutile varied between 1800 and 1870 °C with the partial pressure of O. The value 1870 °C corresponded to stoichiometric rutile [72Roy]. Other optical pyrometry on the melting point gave values ranging between 1825 and 1850 °C, (see Table 2 [75Cha]). According to [60Bra] and [72Roy], these measurements pertained to slightly reduced rutile.

The liquidus between Ti₂O₃ and TiO₂ was determined under argon at 10⁵ Pa [60Bra]. Between Ti₂O₃ and TiO₂, at least one eutectic reaction must occur; [60Bra] and [56Nis] agreed that the reaction is $L \rightleftharpoons \beta$ Ti₂O₃ + TiO₂ at 1670 ± 15 °C.

If the above interpretation is correct, the intermediate Magneli phases decompose by solid-state reactions below 1670 °C. Incongruent melting points were reported for

β Ti₃O₅ and γ Ti₄O₇ (Table 2), but [65Por] claimed to have shown that the Magneli phases are stable until they melt. On the basis of their O-potential measurements, [74Gre] and [83Zad] presented a more complicated picture. According to [74Gre], the Magneli phases with *n* odd are less stable than those with *n* even. [83Zad] verified this for Ti₇O₁₃ and Ti₉O₁₇, which were not observed as single phase above 1500 °C. From O-potential data and XRD, [83Zad] concluded tentatively that γ Ti₄O₇ is unstable with respect to β Ti₃O₅ and Ti₅O₉ above 1500 °C.

This assessment accepts the temperature value 1670 ± 15 °C for a eutectic reaction involving unknown solid phases. On the basis of liquidus data [60Bra], a peritectic reaction β Ti₂O₃ + L \rightleftharpoons β Ti₃O₅, is shown in the assessed diagram. The fact that ~1670 °C is the best value reported for the melting temperature of γ Ti₄O₇ [71Ham] is consistent with the hypothesis that, on heating, γ Ti₄O₇ first decomposes in the solid state and then melts by a eutectic reaction.

Magneli Phases. In early work, the region including the Magneli phases was identified as a single phase of wide homogeneity range [39Ehr]. The Magneli phases, or crystallographic shear structures, were established later as discrete, stoichiometric equilibrium phases, Ti_{*n*}O_{2*n*-1}, both by structural studies [57And1] and by oxygen-potential measurements [64Roy, 73Mer, 83Zad]. The contrary assertion by [63Bog] was regarded by [70And] as a misinterpretation of the tensimetric data. In addition to the series (4 ≤ *n* ≤ 10), other families of structures based on other shear planes were established [69Bur, 70And, 71Bur1, 71Bur2]. Some estimates of the largest value of

Table 6 Ti-O Lattice Parameter Data

Phase	Composition, at.% O	Lattice parameters, nm			Angle		γ	Reference	
		a	b	c	α	β			
Ti ₃ O	25	0.51411	...	0.95334		[71Dub1, 71Dub2]	
		0.506	...	0.956		[70Kor]	
		0.506	...	0.948		[70Kor]	
Ti ₂ O	33.3	0.29593	...	0.48454		[71Dub1, 71Dub2]	
		0.29593	...	0.48454		[62Hol]	
		0.296	...	0.483		[70Kor]	
Ti ₃ O ₂	~40	0.49915	...	0.28794		[59And]	
β TiO	50	1.254		[68Hil1]	
α TiO	50	0.5855	0.9340	0.4142	...	107.53°		[67Wat]	
		0.9355	0.5868	0.4135	...	107.53°		[68Hil2]	
β Ti _{1-x} O	...	0.2981	0.9086	0.3986		[66Wat, 68Hil1]	
α Ti _{1-x} O	...	0.6594	...	0.4171		[68Wat]	
α Ti ₂ O ₃ (a)	60	0.6632	...	0.4156		[68Hil1]	
		0.5431	56.58°	...		[62Str]	
		0.6632	...	0.4156		[68Hil1]	
		59.8	0.5160	56.80°	...		[57And2]
		60.0	0.5425	56.73°	...		
		60.2	0.5432	56.56°	...		
		60	0.542	56.9°	...		[61Mag]
		60	0.5428	56.65°	...		[58Pea]
		60	0.543258	56.75°	...		[74Rob]
		β Ti ₃ O ₅	62.5	0.982	0.378	0.997	...	91.0°	
		0.9484	0.3755	0.9735	...	90.0°		[51Rus]	
		0.9828	0.3776	0.9898	...	91.32°		[69Iwa]	
		0.990	0.378	1.002	...	90.75°		[71Rao]	
α Ti ₃ O ₅	62.5	0.9757	0.3802	0.9452	...	93.11°		[57Asb, 57And2]	
		0.97524	0.38020	0.94419	...	91.547°		[61Mag]	
		0.976	0.380	0.943	...	91.58°		[69Iwa]	
		0.9752	0.38020	0.9442	...	91.55°		[59Asb]	
		0.980	0.379	0.945	...	91.75°		[71Rao]	
α' Ti ₃ O ₅	62.5	1.0120	0.5074	0.9970	...	138.15°		[71Asb]	
γ Ti ₄ O ₇	63.6	0.5604	0.7137	1.2478	95.072°	95.16°	108.77°	[63And]	
		0.5593	0.7125	1.2456	95.02°	95.21°	108.73°	[73Mer]	
		0.5600	0.7133	1.2466	95.05°	95.17°	108.71°	[71Mar]	
		0.5593	0.7125	2.043	67.63°	57.17°	108.73°	[82Lep1]	
β Ti ₄ O ₇	63.6	0.5590	0.7128	1.2483	95.03°	95.34°	108.89°	[73Mer]	
		0.6918	1.1142	1.5127	90.64°	92.79°	91.45°	[84Lep](b)	
α Ti ₄ O ₇	63.6	0.5591	0.7131	1.2487	95.00°	98.33°	108.88°	[73Mer]	
		0.5626	0.7202	2.0260	67.90°	57.69°	109.68°	[84Lep](b)	
β Ti ₅ O ₉	64.3	0.5569	0.7120	0.8865	97.55°	112.34°	108.50°	[60And]	
		0.5577	0.7117	2.632	67.24°	57.04°	108.51°	[77Mar](b)	
γ Ti ₆ O ₁₁	64.7	0.5566	0.7144	2.407	98.5°	120.8°	108.5°	[61And]	
		0.5552	0.7126	3.2234	66.94°	57.08°	108.50°	[82Lep1]	
β Ti ₇ O ₁₃	65.0	0.554	0.713	1.536	98.9°	125.5°	108.5°	[61And]	
		0.5537	0.7132	3.8152	66.70°	57.12°	108.50°	[82Lep1]	
β Ti ₈ O ₁₅	65.2	0.557	0.710	3.746	97.2°	128.8°	109.6°	[61And]	
		0.55261	0.7133	4.4060	66.54°	57.18°	108.51°	[82Lep1](b)	
β Ti ₉ O ₁₇	65.4	0.55272	0.71413	2.22788	99.26°	130.34	108.50°	[61And]	
		0.55241	0.71421	5.0031	66.41°	57.20°	108.53°	[82Lep1](b)	
Rutile	66.667	0.4594	...	0.2959		[56Bau]	
		0.4593	...	0.2959		[57And2]	
		0.45929	...	0.29591		[55Cro]	
		0.459373	...	0.295812		[61Str]	
Anatase	66.7	0.3786	...	0.9517		[57And2]	
		0.3785	...	0.9514		[55Cro]	
Brookite	66.7	0.925	0.546	0.516		[61Yog]	
		0.9184	0.5447	0.5145		[59Wey]	
TiO ₂ -II	66.7	0.4515	0.5497	0.4939		[67Sim]	
		0.4529	0.5464	0.4905		[67Mcq]	
		0.4531	0.5498	0.4900		[66Ben]	
TiO ₂ -III	66.7	0.922	...	0.5685		[78Liu]	

Note: At room temperature. (a) Temperature-dependent lattice parameters were determined by [68Rao] and [58Pea]. (b) See text for a description of the cell.

n were 36 [72Por] and 40 [70And]. [65Por] and [72Roy] suggested that the largest value may be as high as 99. The lower estimates, based on structural data, are probably more realistic.

The assessed diagram, Fig. 1, displays the Magneli phases with stoichiometries Ti₄O₇ through Ti₇O₁₃. Additional members of this family and other families, produced by different crystallographic shear operations, were shown to be possible theoretically and demonstrated experimentally [69Bur, 70And, 71Bur1, 71Bur2]. There is some evi-

dence that higher index crystallographic shear structures are stable only at lower temperatures [71Bur2].

Modifications of Ti₂O₃. The homogeneity range of β Ti₂O₃ (59 to 61 at.% O), reported by [39Ehr], was widely quoted; a narrower range (59.8 to 60.2 at.% O), based on lattice parameter data [57And1], is preferred.

Ti₂O₃ undergoes a transition from semiconducting α Ti₂O₃ at low temperature to metallic β Ti₂O₃ at about 180 °C. There has been some disagreement concerning the mecha-

nism and temperature of the transition (see Table 3). [58Pea] and [68Rao] found rapid changes in the dimensions of the unit cell between 160 and 200 and between 117 and 177 °C, respectively, but no symmetry change. [63Abr] reported that antiferromagnetic $\alpha\text{Ti}_2\text{O}_3$ with monoclinic symmetry changed to rhombohedral $\beta\text{Ti}_2\text{O}_3$; other investigators reported only a distension of the rhombohedral unit cell [58Pea, 68Rao]. [46Nay] found an effect in the heat content at 200 ± 20 °C and [73Bar] found a λ -type peak in the heat capacity at 180 °C. In approximate agreement, [67Key1] and [67Key2] found a change in the magnetic susceptibility at about 130 °C. On the other hand, [63Abr], by neutron diffraction, found that antiferromagnetic ordering occurred below 390 ± 30 °C and connected it with a change in electrical resistivity occurring over the range 180 to 630 °C.

In the present assessment, the thermochemical and lattice parameter data are preferred tentatively as indicators of the phase transition, which is placed at 180 °C.

Modifications of Ti_3O_5 . This phase has at least two equilibrium modifications: $\alpha\text{Ti}_3\text{O}_5$, stable below about 190 °C [59Asb, 71Rao]; and the high-temperature form, $\beta\text{Ti}_3\text{O}_5$, (anosovite), probably stable to the melting point [51Rus, 59Asb]. The $\beta\text{Ti}_3\text{O}_5 \rightleftharpoons \alpha\text{Ti}_3\text{O}_5$ transition occurs with a hysteresis of about 30 °C [71Rao]. Experimental data on the transition temperatures are listed in Table 3. The transition is from a metallic conductor to a semiconductor. $\beta\text{Ti}_3\text{O}_5$ was stabilized to room temperature by Fe impurities [59Asb, 71Rao].

[72Roy] reported an additional phase transition at about 1200 °C. The basis for its inclusion was not specified; consequently it has been omitted from the assessed diagram. Another structural modification, $\alpha'\text{Ti}_3\text{O}_5$, formed at 600 to 925 °C [71Asb], but because of the irreversibility of the $\alpha'\text{Ti}_3\text{O}_5 \rightarrow \alpha\text{Ti}_3\text{O}_5$ transformation, $\alpha'\text{Ti}_3\text{O}_5$ has been considered metastable. [69Iwa] identified three forms of Ti_3O_5 that they designated *D*, *D'*, and *M*. Structurally, the *D* and *D'* probably could be identified as $\beta\text{Ti}_3\text{O}_5$ and *M* as $\alpha\text{Ti}_3\text{O}_5$. [69Iwa] distinguished the three forms according to the products of oxidation under different conditions (rutile or a mixture of anatase and rutile). The *D* type was thought to be metastable.

Modifications of Ti_4O_7 . This phase undergoes two transitions: $\gamma\text{Ti}_4\text{O}_7 \rightleftharpoons \beta\text{Ti}_4\text{O}_7$ at 150 K and $\beta\text{Ti}_4\text{O}_7 \rightleftharpoons \alpha\text{Ti}_4\text{O}_7$ at 125 K, which bring it from a metallic conductor at room temperature to an insulator below 125 K [69Bar, 70Mar, 73Mar]. [70Mar] observed the upper transition only from a discontinuity in the lattice parameters; at the lower transition, new X-ray reflections were observed [69Bar, 70Mar]. [73Mar] reported that when purer samples were used, both transitions involved only the rearrangement of atoms within the unit cell. [84Lep] verified the structures of $\gamma\text{Ti}_4\text{O}_7$ and $\alpha\text{Ti}_4\text{O}_7$, but attributed to $\beta\text{Ti}_4\text{O}_7$ a five-fold increase in the cell size.

Modifications of Ti_5O_9 and Higher Magneli Phases. Ti_5O_9 , Ti_6O_{11} , Ti_7O_{13} , Ti_8O_{15} , Ti_9O_{17} , and $\text{Ti}_{10}\text{O}_{19}$ were shown similarly to undergo electrical transitions. In Ti_5O_9 , two transitions occurred very close together [69Bar]. The higher Magneli phases were studied more cursorily, but they appear to have transitions at approximately 150 K [67Key1, 67Key2, 70Mul]. Data are summarized in Table 3. In magnetic susceptibility studies, measurements extended to a

sharp change, suggestive of another phase transition [72Dan].

TiO_2 (Rutile). Five polymorphs of TiO_2 exist: anatase and brookite, which are low-temperature, low-pressure forms; $\text{TiO}_2\text{-II}$ and $\text{TiO}_2\text{-III}$, which are formed from anatase or brookite under pressure; and rutile, the stable phase at all temperatures and ambient pressure. The polymorphic transformations anatase \rightarrow rutile and brookite \rightarrow rutile do not occur reversibly [66Vah, 68Dac]. This fact and the heat of transformation data [67Nav, 79Mit] showed that anatase and brookite are not stable at any temperature. Therefore, in the assessed phase diagram (Fig. 1), only rutile is shown. Temperature-pressure data for the polymorphic transformations are discussed in the section "Metastable Phases."

Experimental data on the homogeneity range of rutile are summarized in Table 4. The tabulated compositions vary between 66.6 at.% O at 1000 °C to about 66.3 at.% O near the melting point. In Fig. 1, TiO_2 is represented simply as a stoichiometric line compound.

Metastable Phases

Terminal Solid Solution, (Ti). Above a critical cooling rate of 3000 °C/s, the (βTi) \rightleftharpoons (αTi) transition is diffusionless, i.e., either martensitic or massive in mechanism. [74Cor] measured the start temperature, M_s , of the (assumed) martensitic transformation as:

Composition, at.% O	M_s , °C
0.....	802 \pm 10
0.6.....	836
0.9.....	861
1.0.....	901
1.2.....	849
1.5.....	832

The maximum in M_s at about 1 at.% O was stated to be real, but its origin was not explained.

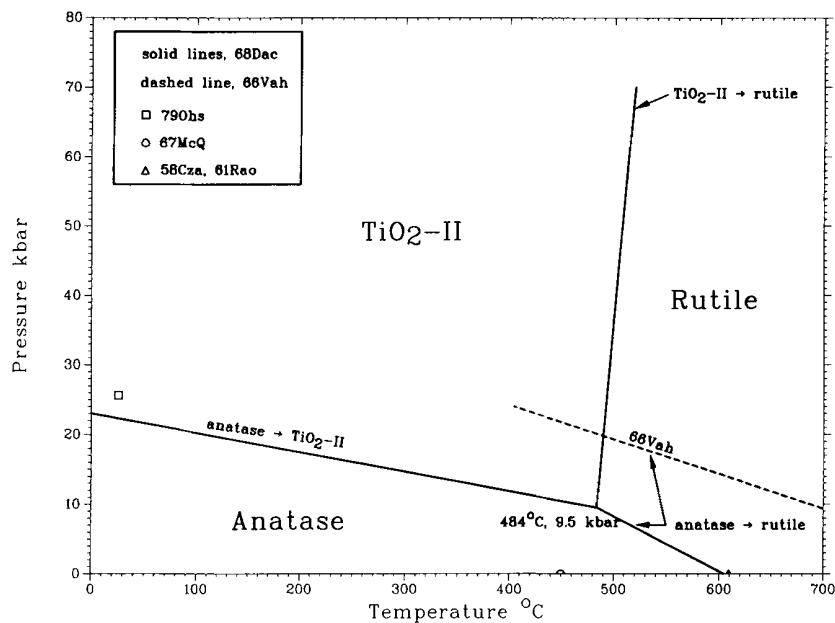
Anatase, Brookite, $\text{TiO}_2\text{-II}$ and $\text{TiO}_2\text{-III}$. As already noted, heat of transformation data and irreversibility of the anatase \rightarrow rutile and brookite \rightarrow rutile transformations indicate that rutile is the stable phase at all temperatures. Similarly, the transformations of anatase and brookite to the high-pressure forms, $\text{TiO}_2\text{-II}$ and $\text{TiO}_2\text{-III}$, occur irreversibly.

The nonequilibrium transformations have been examined experimentally:

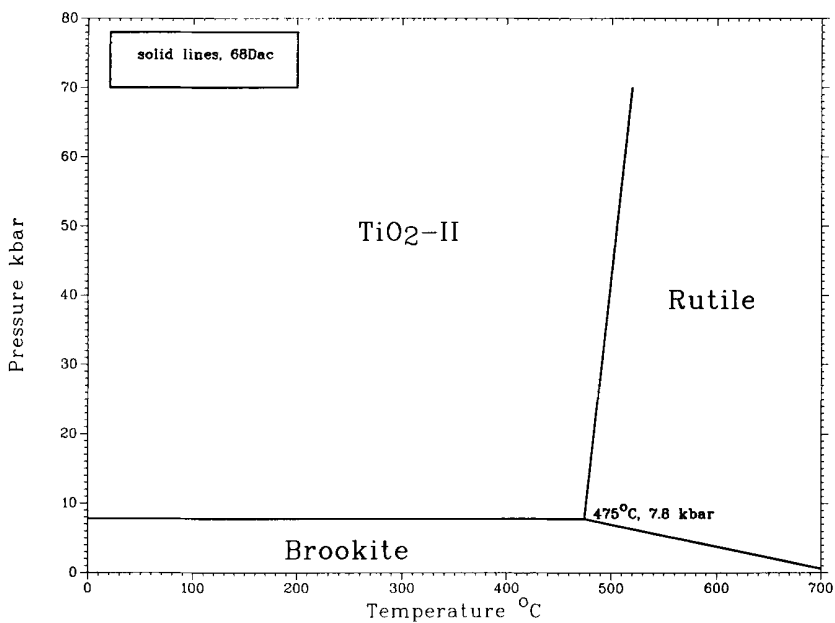
Transformation	References
Anatase \rightarrow rutile.....	[58Cza, 61Rao, 66Vah, 68Dac]
Brookite \rightarrow rutile.....	[68Dac]
$\text{TiO}_2\text{-II} \rightarrow$ rutile.....	[68Dac, 66Ben]
$\text{TiO}_2\text{-II} \rightarrow \text{TiO}_2\text{-III}$	[67Mcq, 78Liu, 81Mam]
Anatase $\rightarrow \text{TiO}_2\text{-III}$	[68Dac, 79Ohs]
Rutile $\rightarrow \text{TiO}_2\text{-II}$	[71Nic, 78Liu, 80Mam, 66Ben]

The transformations anatase \rightarrow rutile, anatase $\rightarrow \text{TiO}_2\text{-II}$, and $\text{TiO}_2\text{-II} \rightarrow$ rutile can be represented in a nonequi-

Fig. 6 Observed Conditions for Persistence or Induced Transformation of Unstable Anatase (or Brookite) and TiO₂-II



(a)



(b)

J.L. Murray and H.A. Wriedt, 1987.

librium temperature-pressure diagram, as can the corresponding transformations with brookite replacing anatase. Figure 6 shows the diagrams determined by [68Dac] with quenching and X-ray techniques in the range 0 to 80 kbar, 200 to 700 °C. In the figure, the data of [58Cza], [61Rao], [66Vah] for the anatase → rutile transformation and of [79Ohs] for the anatase to TiO₂-II transformation are compared with the results of [68Dac].

The diagrams in Fig. 6 are neither stable nor metastable equilibrium diagrams from which heats of transformation could be calculated. They indicate conditions for which the rate of transformation in the appropriate direction is appreciable. Of the high-pressure phases, TiO₂-II is formed more easily and is the only one that can be retained during quenching.

The kinetics of the anatase → rutile transformation were studied by [58Cza], who used X-ray spectroscopy as a probe of the volume fractions of the phases and found that the transformation occurred infinitely slowly at 610 °C. [61Rao] extrapolated thermal analysis data to zero heating rate to obtain a transformation temperature of 610 ± 10 °C. [66Vah] examined the transition by electrical resistivity measurements in samples quenched from 3.8 to 24 kbar, and 20 to 1000 °C. Transformation of rutile to TiO₂-II occurs at pressures above 7 GPa [71Nic, 78Liu, 80Mam] and temperatures above about 700 °C [66Ben]. The transformation of TiO₂-II to TiO₂-III at about 20 to 30 GPa was observed with XRD and Raman spectroscopy [67Mcq, 78Liu, 81Mam]. The crystallographic mechanisms of these transformations were examined by [64Sha] and [70Sim2].

Table 7 Lattice Parameters of Dilute (α Ti) Alloys at 21 °C

Composition, at. ppm O	Lattice parameters, nm	
	<i>a</i>	<i>c</i>
90	0.295112	0.468272
...	0.295135	0.468288
...	0.295126	0.468243
300	0.295129	0.468299
1026	0.295121	0.468315
1336	0.2956162	0.468369
1900	0.295142	0.468435
2332	0.295138	0.468434
...	0.295182	0.468462
3104	0.295149	0.468458
...	0.295133	0.468465
...	0.295226	0.468515

From [77Dec].

Table 8 Thermodynamic Properties of Intermetallic Phases

Phase	Entropy of formation (a) ($\Delta_f S^\circ$), kJ/mol·K	Enthalpy of formation (a) ($\Delta_f H^\circ$), kJ/mol	Enthalpy of fusion ($\Delta_{fus} H$), kJ/mol	Enthalpy of transition ($\Delta_{trs} H$), kJ/mol
α TiO	34.77 ± 2	-542.7 ± 12
β TiO	38.1	-538.5 ± 12	41.8	...
β Ti ₂ O ₃	77.24 ± 0.2	-1520.9 ± 8	104.6	...
α Ti ₃ O ₅	129.37	-2459.15 ± 4	...	13.26 ± 6.3
β Ti ₃ O ₅	157.620	-2446.188	177	...
β Ti ₄ O ₇	198.7 ± 12	-3404.5 ± 6.3	266	...
Anatase	49.907 ± 0.3	-938.72 ± 2	57.99	...
Rutile	50.29 ± 0.17	-939.89 ± 1.2	66.9 ± 17	...

From [75Cha].
(a) At 25 °C.

Crystal Structures and Lattice Parameters

Tables 5 and 6 contain crystal structure and room temperature lattice parameter data on the observed phases of the Ti-O system; those phases that are probably not equilibrium binary phases at low pressure are distinguished by footnotes. For the Magneli phases, comparison of lattice parameters from various authors has been made by application of the cell transformations, described below.

Measurements of the lattice parameter of (α Ti) as a function of composition are shown in Fig. 7. The values for very dilute alloys are listed in Table 7. Because (β Ti) could not be retained by quenching, its lattice parameters were not measured.

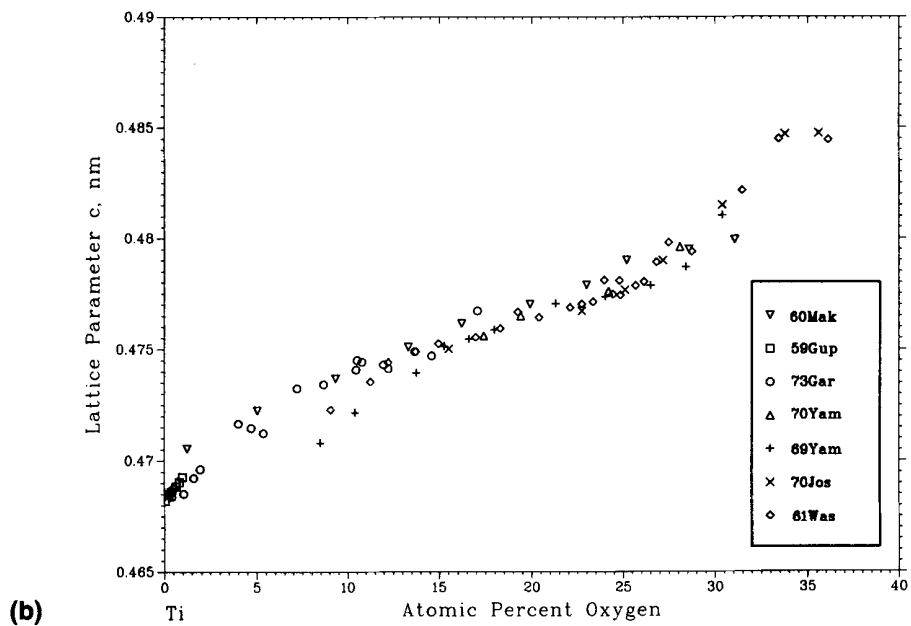
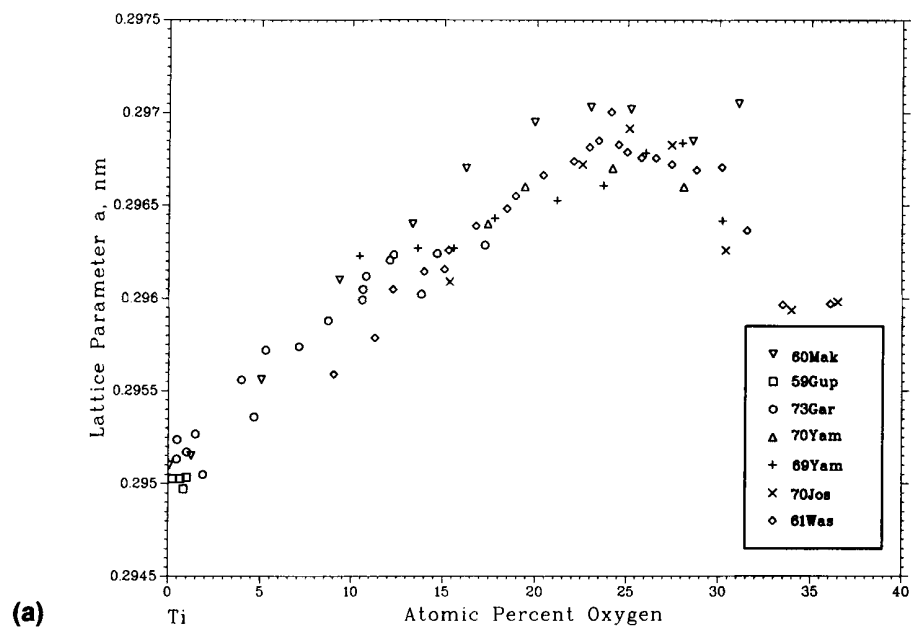
The structures of Ti₂O and Ti₃O and their relationships are discussed above. Note that the early structure determinations of Ti₆O [66Yam] and Ti₃O [68Jos] are not listed, because they were superseded by later work, including neutron diffraction [69Yam, 70Kor, 70Yam, 71Dub1, 71Dub2].

γ TiO has the NaCl structure [39Ehr]; lattice parameter values are shown in Fig. 8. Other forms of the monoxide — β TiO, α TiO, β Ti_{1-x}O, and α Ti_{1-x}O — have ordered structures based on γ TiO. The intermediate-temperature phase β TiO identified by [68Hil1] is cubic with a lattice parameter three times that of the γ TiO parameter. The structure of the equilibrium low-temperature form α TiO was determined by [67Wat] and [68Hil1]. In every third (110) _{γ TiO} plane, half the O and half the Ti atoms were missing, in ordered fashion. The ordered orthorhombic structure β Ti_{1-x}O was identified in thin foils for Ti-rich compositions [65Wat, 69Ver] and for O-rich compositions [68Hil1]. The structure differs from that of α TiO in that only the O vacancies were ordered.

The high-temperature β Ti₃O₅ phase was reported originally to be orthorhombic [51Rus]; the accepted monoclinic structure is a slight distortion of the orthorhombic lattice. The effect of impurities is to lessen the distortion [59Asb]. The names "anosovite" and "pseudobrookite" refer to the β Ti₃O₅ structure.

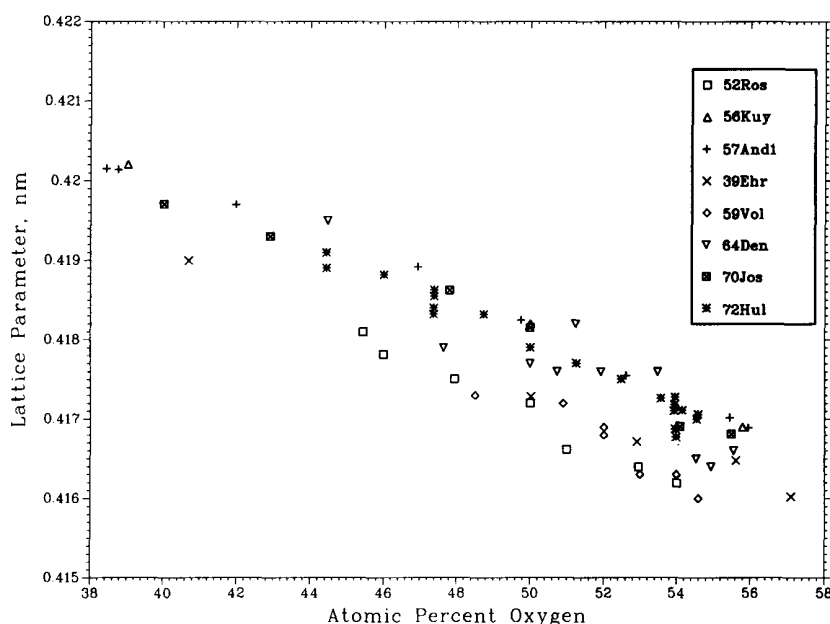
Several choices were made for the cell upon which to index the structures of the Magneli phases, Ti_nO_{2n-1} for 4 ≤ n ≤ 9 [63And, 82Lep1]. One choice was the rutile cell and another was the following: for odd n, the cell is primitive, for even n, the cell is A face centered [61And, 73Mar]. [82Lep1] chose a nonconventional body-centered cell, which allows a more convenient comparison of the various structures. The relationship among the rutile (R), [61And] (A), and [82Lep1] (L) cells was given by [82Lep1]:

Fig. 7 Experimental Measurements of the Variation of the Lattice Parameters of cph (α Ti) with O Concentration



J.L. Murray and H.A. Wriedt, 1987.

Fig. 8 Experimental Measurements of the Variation of the Lattice Parameter of γ TiO with O Concentration



J.L. Murray and H.A. Wriedt, 1987.

$$a_L = a_A = a_R - c_R$$

$$b_L = b_A = -a_R - b_R - c_R$$

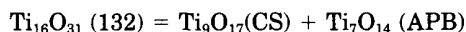
$$c_L = (2n - 5)a_A + (n - 2)b_A + pc_A = -(2n - 1)c_R$$

where $p = 1$ for n even and $p = 2$ for n odd.

In Tables 5 and 6, symmetry and lattice parameter data are as listed originally by the authors.

[63And] and [67And] described the structures of the Magneli phases as derivatives of the rutile structure by the following crystallographic operations: every $2n^{\text{th}}$ O plane parallel to $(121)_{\text{rutile}}$ was removed to adjust the composition, and adjacent rutile slabs were displaced by $1/2(011)_{\text{rutile}}$ to collapse the structure.

More complex structures appeared in higher oxides. [69Bur] and [71Bur1] described another family of oxides with the same generic formula $\text{Ti}_n\text{O}_{2n-1}$ that were generated by the removal of the $(132)_{\text{rutile}}$ O planes. Phases were identified for $16 \leq n$ (even) ≤ 36 [71Bur1, 71Bur2]. [71Bur2] resolved the crystallographic operations into combinations of a (121) operation (which altered the composition) and the introduction of a (011) antiphase boundary. The (132) structure was described as an ordered coherent intergrowth structure of crystallographic shear (CS) and antiphase boundary (APB) structures:



In this way, new families of generic shear structures were derived. The existence of (253) -type crystallographic shear structure was verified by electron diffraction [71Bur2].

Table 9 Heats of Formation of Oxides at 1400 °C

Phase	Heat of formation, ($\Delta_f H$), kJ/mol	Phase	Heat of formation, ($\Delta_f H$), kJ/mol
Ti_3O_5	-2414	Ti_7O_{13}	-6130
Ti_4O_7	-3351	Ti_8O_{15}	-7054
Ti_5O_9	-4276	Ti_9O_{17}	-7979
Ti_6O_{11}	-5212	$\text{Ti}_{10}\text{O}_{19}$	-8912

Note: Mol is mole of atoms. From [83Zad].

The temperature dependence of the lattice parameters of $\gamma\text{Ti}_4\text{O}_7$ and $\beta\text{Ti}_4\text{O}_7$ was examined by [70Mar].

Thermodynamics

Because the thermodynamic data on the Ti-O system were reviewed extensively [75Cha], the present coverage is restricted to a summary of selected previous assessments and a literature survey of experimental work since 1975.

[75Cha] updated [71Stu] for the Ti-O system, covering the solid phases βTiO , αTiO , $\beta\text{Ti}_2\text{O}_3$, Ti_4O_7 , $\beta\text{Ti}_3\text{O}_5$, $\alpha\text{Ti}_3\text{O}_5$, TiO_2 (anatase), TiO_2 (rutile), and the liquids at corresponding compositions. Heats and entropies of formation of the compounds from the pure elements in their standard states are given in Table 8.

[64Kau] analyzed thermochemical data for the interstitial solutions (αTi) and (βTi) and the monoxide γTiO . Data for nonstoichiometric compositions of the compound were analyzed in terms of the Wagner-Schottky model; a general model was presented for interstitial solid solutions, with a variable number of available interstitial sites. Compari-

O-Ti

son was made between observed and calculated values of the enthalpy of formation and vacancy concentration of γ TiO as a function of composition. It was stated that the calculated (α Ti)/(β Ti) phase boundaries were within 2 at.% of the assessed boundaries of [Hansen].

The following is recent experimental work:

- High-temperature O activities on the O-rich side of the diagram were measured by [78Koz], [82Gra], and [83Zad]. Heats of formation derived by [83Zad] are listed in Table 9.
- High-temperature partial heats of formation were measured for compositions near TiO₂ and TiO [75Pic, 76Bou, 78Tet, 81Tet]. [78Tet] corrected previous work [76Bou]. The results differed from previous work, and appeared also to differ from the present assessed phase diagram.
- Relative partial Gibbs energies for dilute (α Ti) solutions were given by [73Rez]. Expressions for relative partial Gibbs energies of O were given for six alloys containing 0.15 to 0.9 at.% O over the range 1000 to 1150 °C.

[79Mit] determined the enthalpy changes for the transformations anatase \rightarrow rutile and brookite \rightarrow rutile as 698 °C by solution calorimetry, supplemented by DSC and DTA:

For $\Delta_{\text{trs}}H$ (anatase \rightarrow rutile):

$$698 \text{ °C} = -3.26 \pm 0.84 \text{ kJ/mol}$$

For $\Delta_{\text{trs}}H$ (brookite \rightarrow rutile):

$$698 \text{ °C} = -0.71 \pm 0.4 \text{ kJ/mol}$$

For $\Delta_{\text{trs}}H$ (anatase \rightarrow rutile):

$$698 \text{ °C} = -2.93 \pm 1.3 \text{ kJ/mol (DSC)}$$

Temperature-pressure transformation data could not be used to determine $\Delta_{\text{trs}}H$, because rutile is the stable phase at all temperatures. [79Mit] attributed the discrepancy between their results and previous solution calorimetry data [67Nav] to failure to dissolve the samples completely in the solvent in the earlier work.

Cited References

- 37Daw:** W. Dawhill and K. Schroter, "Preparation and Properties of Titanium Monoxide," *Z. Anorg. Chem.*, **233**, 178-183 (1937). (Equi Diagram; Experimental)
- 39Ehr:** P. Ehrlich, "Phase Relations and Magnetic Properties in the Titanium-Oxygen System," *Z. Electrochem.*, **45**, 362-370 (1939) in German. (Equi Diagram; Experimental)
- 46Nay:** B.F. Naylor, "High-Temperature Heat Contents of TiO, Ti₂O₃, Ti₃O₅, and TiO₂," *J. Amer. Chem. Soc.*, **68**, 1077-1068 (1946). (Equi Diagram; Experimental)
- 50Jaf:** R.I. Jaffee, H.R. Ogden, and D.J. Maykuth, "Alloys of Titanium with Carbon, Oxygen, and Nitrogen," *Trans. Metall. AIME*, **188**, 1261-1266 (1950). (Equi Diagram; Experimental)
- *51Jen:** A.E. Jenkins and H.W. Worner, "The Structure and Some Properties of Titanium-Oxygen Alloys Containing 0-5 at. Percent Oxygen," *J. Inst. Met.*, **80**, 157-166 (1951). (Equi Diagram, Experimental)
- 51Rus:** A.A. Ruskov and G.S. Ladanov, "Crystal Structure and Stoichiometry of Ti₃O₅ (Anosovite)," *Dokl. Akad. Nauk SSSR*, **77**, 411-414 (1951) in Russian. (Equi Diagram, Crys Structure; Experimental)
- 52Ros:** W. Rostoker, "Observations on the Lattice Parameters of the Alpha and TiO Phases in the Titanium-Oxygen System," *Trans. Metall. AIME*, **194**, 981-982 (1952). (Crys Structure; Experimental)
- *53Bum:** E.S. Bumps, H.D. Kessler, and M. Hansen, "The Titanium-Oxygen System," *Trans. Metall. AIME*, **45**, 1008-1028 (1953). (Equi Diagram; Experimental)
- 54Dev:** R.C. DeVries, R. Roy, and E.F. Osborn, "The System TiO₂-SiO₂," *Trans. J. Brit. Ceram. Soc.*, **53**, 525-540 (1954). (Equi Diagram; Experimental)
- 54Kub:** O. Kubaschewski and W.A. Dench, "The Free-Energy Diagram of the System Titanium-Oxygen," *J. Inst. Met.*, **82**, 87-91 (1954). (Equi Diagram, Thermo; Experimental)
- 54Was:** R.J. Wasilewski and G.L. Kehl, "Diffusion of Nitrogen and Oxygen in Titanium," *J. Inst. Met.*, **83**, 94-104 (1954). (Equi Diagram; Experimental)
- 55Cro:** D.T. Cromer and K. Herrington, "The Structures of Anatase and Rutile," *J. Am. Chem. Soc.*, **77**, 4708-4709 (1955). (Crys Structure; Experimental)
- 56Bau:** W.H. Baur, "Determination of Refined Crystal Structure for Several Compounds of the Rutile Type: TiO₂, SnO₂, GeO₂ and MgF₂," *Acta Crystallogr.*, **9**, 515-520 (1956). (Crys Structure; Experimental)
- 56Kuy:** U. Kuylenstierna and A. Magneli, "A New Modification of Titanium Monoxide," *Acta Chem. Scand.*, **10**(7), 1195-1196 (1956). (Equi Diagram, Crys Structure; Experimental)
- 56Nis:** H. Nishimura and H. Kimura, "On the Equilibrium Diagram of Titanium-Oxygen-Carbon System (II). The Titanium-Oxygen System," *J. Jpn. Inst. Met.*, **20**, 524-527 (1956) in Japanese. (Equi Diagram; Experimental)
- *56Sch:** T.H. Schofield, "The Constitution of the Titanium-Oxygen Alloys in the Range 0.35 Weight Per Cent Oxygen," *J. Inst. Met.*, **84**, 47-53 (1956). (Equi Diagram; Experimental)
- 56Wan:** C.C. Wang and N.J. Grant, "Transformation of the TiO Phase," *J. Met.*, **8**, 184-185 (1956). (Equi Diagram; Experimental)
- *57And1:** S. Andersson, B. Collen, U. Kuylenstierna, and A. Magneli, "Phase Analysis Studies on the Titanium-Oxygen System," *Acta Chem. Scand.*, **11**, 1641-1652 (1957). (Equi Diagram, Crys Structure; Experimental)
- 57And2:** S. Andersson, B. Collen, G. Kruse, U. Kuylenstierna, A. Magneli, H. Pestmalis, and S. Asbrink, "Identification of Titanium Oxides by X-Ray Powder Patterns," *Acta Chem. Scand.*, **11**, 1653-1657 (1957). (Crys Structure; Experimental)
- 57Asb:** S. Asbrink and A. Magneli, "Note on the Crystal Structure of Trititanium Pentoxide," *Acta Chem. Scand.*, **11**(9), 1606-1607 (1957). (Crys Structure; Experimental)
- 57Kon:** I. Koncz and M. Koncz-Deri, "Formation of the Delta-Phase by Oxidation of Alpha-Titanium," *Period. Polytech.*, **1**, 67-87 (1957). (Equi Diagram; Experimental)
- 57Mah:** A.D. Mah, K.K. Kelley, N.L. Gellert, E.G. King, and C.J. O'Brien, "Thermodynamic Properties of Titanium-Oxygen Solutions and Compounds," *Bur. Mines Rep. Invest.* 5316 (1957). (Equi Diagram, Thermo; Experimental)
- 58Cza:** A.W. Czanderna, C.N.R. Rao, and J.M. Honig, "The Anatase-Rutile Transition Part 1. - Kinetics of the Transformation of Pure Anatase," *Trans. Faraday Soc.*, **54**, Part 7, 1067-1073 (1958). (Meta Phases; Experimental)
- 58Pea:** A.D. Pearson, "Studies on the Lower Oxides of Titanium," *J. Phys. Chem. Solids*, **5**, 316-327 (1958). (Equi Diagram, Crys Structure; Experimental)
- 59And:** S. Anderson, "The Crystal Structure of the So-Called Alpha-Titanium Oxide and Its Structural Relation to the Omega-Phases of Some Binary Alloy Systems of Titanium," *Acta Chem. Scand.*, **13**, 415-419 (1959). (Equi Diagram, Crys Structure; Experimental)
- 59Asb:** S. Asbrink and A. Magneli, "Crystal Structure Studies on Trititanium Pentoxide, Ti₃O₅," *Acta Crystallogr.*, **12**, 575-581 (1959). (Equi Diagram, Crys Structure; Experimental)
- 59Gup:** D. Gupta and S. Weing, "The Dislocation-Oxygen Interaction in Alpha Titanium and Its Effect on the Ductile-to-Brittle Transition," *Trans. Metall. AIME*, **215**, 209-216 (1959). (Crys Structure; Experimental)
- 59Now:** H. Nowotny and E. Dimakopoulou, "The Ti₂O Phase," *Monatsh. Chem.*, **90**, 620-622 (1959) in German. (Crys Structure; Experimental)
- 59Vol:** E. Volf, S.S. Tolkachev, and I.I. Kozhina, "X-Ray Study of the Lower Oxides of Titanium and Vanadium," *Vestn. Leningrad Univ.*, **14**(10), Ser. Fiz. Khim., (2), 87-92 (1959) in Russian. (Equi Diagram, Crys Structure; Experimental)

- 59Wey:** B. Weyl, "Precision Determination of the Crystal Structure of Brookite, TiO_2 ," *Z. Krist.*, *111*, 401-420 (1959) in German. (Crys Structure; Experimental)
- 59Yao:** Y.L. Yao, "Magnetic Susceptibilities of Titanium-Rich Titanium-Oxygen Alloys," *Trans. Metall. AIME*, *215*, 851-854 (1959). (Equi Diagram; Experimental)
- 60And:** S. Andersson, "The Crystal Structure of Ti_5O_9 ," *Acta Chem. Scand.*, *14*, 1161-1172 (1960). (Crys Structure; Experimental)
- 60Ari:** S.M. Ariya and N.I. Bogdanova, "Electrical Conductivity of Certain Titanium and Vanadium Oxides," *Sov. Phys. Solid State*, (1), 936-939 (1960). (Equi Diagram; Experimental)
- *60Bra:** G. Brauer and W. Littke, "Melting Point and Thermal Dissociation of Titanium Dioxide," *J. Inorg. Nucl. Chem.*, *16*, 67-76 (1960) in German. (Equi Diagram; Experimental)
- 60Bri:** N.F.H. Bright, "X-Ray Studies in the Ti-O System," *Adv. X-Ray Anal.*, *4*, 175-193 (1960). (Equi Diagram; Experimental)
- 60Mak:** E.S. Makarov and L.M. Kuzneov, *Zh. Strukt. Khim.*, *1*(2), 170-177 (1960) in Russian. (Crys Structure; Experimental)
- 61Mag:** A Magneli, S. Andersson, S. Asbrink, S. Westman, and B. Holmberg, "Crystal Chemistry of Titanium, Vanadium, and Zirconium Oxides at Elevated Temperatures," U.S. Dept. Comm., Office Tech. Serv., PB Rep. 145-923, 82 (1961). (Crys Structure; Experimental)
- 61Rao:** C.N.R. Rao, "Kinetics and Thermodynamics of the Crystal Structure Transformation of Spectroscopically Pure Anatase to Rutile," *Can. J. Chem.*, *39*, 498-500 (1961). (Meta Phases; Experimental)
- 61Str:** M.E. Straumanis, T. Ejima, and W.J. James, "The TiO_2 Phase Explored by the Lattice Constant and Density Method," *Acta Crystallogr.*, *14*, 493-497 (1961). (Equi Diagram, Crys Structure; Experimental)
- 61Was:** R.J. Wasilewski, "Thermal Expansion of Titanium and Some Ti-O Alloys," *Trans. Metall. AIME*, *221*, 1231-1235 (1961). (Crys Structure; Experimental)
- 61Yog:** S.R. Yoganasimhan and C.N.R. Rao, "Titanium Dioxide (Brookite), TiO_2 ," *Anal. Chem.*, *33*(1), 155 (1961). (Crys Structure; Experimental)
- 62Hol:** B. Holmberg, "Disorder and Order in Solid Solutions of Oxygen in Alpha-Titanium," *Acta Chem. Scand.*, *16*, 1245-1250 (1962). (Experimental)
- 62New:** R.E. Newnham and Y.M. De Haan, "Refinement of the Alpha Al_2O_3 , V_2O_3 and Cr_2O_3 Structures," *Z. Krist.*, *117*, 235-237 (1962). (Crys Structure; Experimental)
- 62Str:** M.E. Straumanis and T. Ejima, "Imperfections within the Phase Ti_2O_3 and its Structure Found by the Lattice Parameter and Density Method," *Acta Crystallogr.*, *15*, 404-409 (1962). (Crys Structure; Experimental)
- 62Was:** R.J. Wasilewski, "Electrical Resistivity of Titanium-Oxygen Alloys," *Trans. Metall. AIME*, *224*, 8-12 (1962). (Experimental)
- 63Abr:** S.C. Abrahams, "Magnetic and Crystal Structure of Titanium Sesquioxide," *Phys. Rev. Lett.*, *130*(6), 2230-2237 (1963). (Equi Diagram, Crys Structure; Experimental)
- 63And:** S. Andersson and L. Jahnberg, "Crystal Structure on the Homologous Series Ti_nO_{2n-1} , V_nO_{2n-1} and Ti_nO_{2n-1} , Cr_2O_{2n-1} ," *Arkiv. Kem.*, *21*, 413-426 (1963). (Crys Structure; Experimental)
- 63Bog:** N.I. Bogdanova, G.P. Pirogovskaya, and S.M. Ariya, "Higher Oxides of Titanium," *Zh. Neorg. Khim.*, *8*, 785-787 (1963); TR: *Russ. J. Inorg. Chem.*, *8*, 401-402 (1963). (Equi Diagram; Experimental)
- 63Blu:** R.N. Blumenthal and D.H. Whitmore, "Thermodynamic Study of Phase Equilibria in the Titanium-Oxygen System within the $TiO_{1.95}$ - TiO_2 Region," *J. Electrochem. Soc.*, *110*(1), 92-93 (1963). (Equi Diagram, Thermo; Experimental)
- 63Kor:** I.I. Kornilov and V.V. Glazova, "Phase Diagrams of Ti_6O and Ti_3O in the Titanium-Oxygen System," *Dokl. Akad. Nauk SSSR*, *150*(2), 313-316 (1963) in Russian. (Equi Diagram; Experimental)
- 63Vas:** Y.V. Vasilev, D.D. Khrycheva, and S.M. Ariya, "Magnetic Susceptibility of the Lower Oxides of Titanium," *Russ. J. Inorg. Chem.*, *8*, 402-404 (1963) in Russian. (Equi Diagram; Experimental)
- 64Den:** S.P. Denker, "Relation of Bonding and Electronic Band Structure to the Creation of Lattice Vacancies in TiO ," *J. Phys. Chem. Solids*, *25*, 1397-1405 (1964). (Crys Structure; Experimental)
- 64Kau:** L. Kaufman and E.V. Clougherty, "Thermodynamic Factors Controlling the Stability of Solid Phases at High Temperatures and Pressures," AIME Metall. Soc. Conf., *Metallurgy at High Pressures and High Temperatures*, Vol. 22, Gordon and Breach, Science Publishers, Inc., NY 322-380 (1964).
- 64Roy:** R. Roy, "Controlled O_2 Including High Oxygen Pressure Studies in Several Transition Metal-Oxygen Systems," *CNRS Colloq. Int.*, (149), 27-33 (1964). (Equi Diagram; Experimental)
- 64Sha:** R.D. Shannon and J.A. Pask, "Topotaxy in the Anatase-Rutile Transformation," *Am. Min.*, *49*, 1707-1717 (1964). (Meta Phases; Experimental)
- 65Kor:** I.I. Kornilov and V.V. Glazova, "Thermal Stability of the Compound Ti_3O in the Oxygen-Titanium System," *Zh. Neorg. Chem.*, *10*(7), 1660-1662 (1965) in Russian; TR: *Russ. J. Inorg. Chem.*, *10*(7), 905-907. (Equi Diagram; Experimental)
- 65Por:** V.R. Porter, "Studies in the Titanium-Oxygen System and the Defect Nature of Rutile," *Diss. Abst.*, *27*(11), 6809 (1965). (Equi Diagram; Experimental)
- 65Wat:** D. Watanabe, "Electron Diffraction Study on the Titanium-Oxygen Alloy System," Int. Conf. Electron Diffraction and Crystal Defects, Melbourne, C3 (1965). (Equi Diagram, Crys Structure; Experimental)
- 66Ben:** N.A. Bendeliani, S.V. Popova, and L.F. Vereshchagin, "New Modification of Titanium Dioxide Obtained at High Pressures," *Geochem. Int.*, *3*(3), 387-390 (1966). (Meta Phases, Crys Structure; Experimental)
- 66Dub:** A. Dubertret and P. Lehr, "Hardness Study of Titanium-Oxygen Alloys," *C.R. Acad. Hebd. Seances Sci.*, *263*, 591-594 (1966) in French. (Experimental)
- 66Vah:** F.W. Vahldiek, "Phase Transition of Titanium Dioxide Under Various Pressures," *J. Less-Common Met.*, *11*, 99-110 (1966). (Equi Diagram, Meta Phases; Experimental)
- 66Wah:** P.G. Wahlbeck and P.W. Gilles, "Reinvestigation of the Phase Diagram for the System Titanium-Oxygen," *J. Am. Ceram. Soc.*, *49*(1), 180-183 (1966). (Equi Diagram; Experimental)
- 66Yam:** S. Yamaguchi, M. Koiwa, and M. Hirabayashi, "Interstitial Superlattice of Ti_6O and Its Transformation," *J. Phys. Soc. Jpn.*, *21*, 2096 (1966). (Crys Structure; Experimental)
- 67And:** J.S. Anderson and B.G. Hyde, "On the Possible Role of Dislocations in Generating Ordered and Disordered Shear Structures," *J. Phys. Chem. Solids*, *28*, 1393-1408 (1967). (Crys Structure; Experimental)
- 67Gil:** P.W. Gilles, K.D. Carlson, J.F. Franzen, and P.G. Wahlbeck, "High-Temperature Vaporization and Thermodynamics of the Titanium Oxides. I. Vaporization Characteristics of the Crystalline Phases," *J. Chem. Phys.*, *46*(7), 2461-2465 (1967). (Equi Diagram; Experimental)
- 67Key1:** L.K. Keys and L.N. Mulay, "Magnetism of the Titanium-Oxygen System," *Jpn. J. Appl. Phys.*, *6*, 122-123 (1967). (Equi Diagram; Experimental)
- 67Key2:** L.K. Keys and L.N. Mulay, "Magnetic-Susceptibility Studies on the Magneli Phases of the Titanium-Oxygen System," *J. Appl. Phys.*, *38*(1), 1466-1404 (1967). (Equi Diagram; Experimental)
- 67Mcq:** R.G. McQueen, J.C. Jamieson, and S.P. Marsh, "Shock-Wave Compression and X-Ray Studies of Titanium Dioxide," *Science*, *155*, 1401-1407 (1967). (Meta Phases; Experimental)
- 67Nav:** A. Navrotsky and O.J. Kleppa, "Enthalpy of the Anatase-Rutile Transformation," *J. Am. Ceram. Soc.*, *50*(11), 626 (1967). (Equi Diagram, Thermo; Experimental)
- 67Sim:** P.Y. Simons and F. Dacheille, "The Structure of TiO_2 II, a High Pressure Phase of TiO_2 ," Part 2, *Acta Crystallogr.*, *23*, 334-335 (1967). (Crys Structure; Experimental)
- 67Wat:** D. Watanabe and J.R. Castles, "The Ordered Structure of TiO ," *Acta Crystallogr.*, *23*, 307-313 (1967). (Equi Diagram, Crys Structure; Experimental)
- 68Dac:** F. Dacheille, P.Y. Simons, and R. Roy, "Pressure-Temper-

- ature Studies of Anatase, Brookite, Rutile and TiO_2 II," *Am. Min.*, 53, 1929-1939 (1968). (Meta Phases; Experimental)
- 68Hil1:** E. Hilti, "New Phases in the Titanium-Oxygen System," *Naturwissenschaften*, 55, 130-131 (1968) in German. (Equi Diagram, Crys Structure; Experimental)
- 68Hil2:** E. Hilti and F. Laves, "X-Ray Investigation of the Low-Temperature Modification of Titanium Monoxide," *Naturwissenschaften*, 55, 131 (1968) in German. (Equi Diagram, Crys Structure; Experimental)
- 68Jos:** A. Jostsons and A.S. Malin, "The Ordered Structure of Ti_3O_5 ," *Acta Crystallogr.*, B24, 211-213 (1968). (Crys Structure; Experimental)
- 68Mod:** M.S. Model and G.Y. Shubina, "Investigations of the Structure and Properties of Solid Solutions of Oxygen in Titanium and Zirconium," *Izv. Akad. Nauk SSSR, Met.*, (6), 143-147 (1968) in Russian; *TR: Russ. Met.*, (6), 97-108 (1968). (Equi Diagram; Experimental)
- 68Rao:** C.N.R. Rao, R.E. Loehman, and J.M. Honig, "Crystallographic Study of the Transitions in Ti_2O_3 ," *Phys. Lett. (A)*, 27(5), 271-272 (1968). (Equi Diagram; Experimental)
- 68Wat:** D. Watanabe, O. Terasaki, A. Jostsons, and J.R. Castles, "The Ordered Structure of $TiO_{1.25}$," *J. Phys. Soc. Jpn.*, 25, 292 (1968). (Crys Structure; Experimental)
- 69Bar:** R.F. Bartholomew and D.R. Frankel, "Electrical Properties of Some Titanium Oxides," *Phys. Rev. Lett.*, 187(3), 828-833 (1969). (Equi Diagram; Experimental)
- 69Bur:** L.A. Bursill, B.G. Hyde, O. Terasaki, and D. Watanabe, "On a New Family of Titanium Oxides and the Nature of Slightly-Reduced Rutile," *Philos. Mag.*, 347-359 (1969). (Crys Structure; Experimental)
- 69Hir:** M. Hirabayashi, M. Koiwa, and S. Yamaguchi, "Interstitial Order-Disorder Transformation in the Titanium-Oxygen System," *Mechanism of Phase Transformations in Crystalline Solids*, Inst. Met., London, 207-211 (1969). (Equi Diagram; Experimental)
- 69Iwa:** H. Iwasaki, N.F.H. Bright, and J.F. Rowland, "The Polymorphism of the Oxide Ti_3O_5 ," *J. Less-Common Met.*, 17, 99-110 (1969). (Equi Diagram, Crys Structure; Experimental)
- 69Koi:** M. Koiwa and M. Hirabayashi, "Interstitial Order-Disorder Transformation in the Ti-O Solid Solutions. II. A Calorimetric Study," *J. Phys. Soc. Jpn.*, 27(4), 801-806 (1969). (Equi Diagram; Experimental)
- 69Ver:** A.W. Vere and R.E. Smallman, "The Structure of the Low-Temperature Modification of Titanium Monoxide," *Mechanism of Phase Transformation in Crystalline Solids*, Inst. Met., London, 212-219 (1969). (Equi Diagram, Crys Structure; Experimental)
- 69Yam:** S. Yamaguchi, "Interstitial Order-Disorder Transformation in the Ti-O Solid Solution. I. Ordered Arrangement of Oxygen," *J. Phys. Soc. Jpn.*, 27(1), 155-163 (1969). (Equi Diagram, Crys Structure; Experimental)
- 70And:** J.S. Anderson and A.S. Khan, "Equilibria of Intermediate Oxides in the Titanium-Oxygen System," *J. Less-Common Met.*, 22, 219-223 (1970). (Equi Diagram; Experimental)
- 70Jos:** A. Jostsons and R. McDougall, "Phase Relationships in Titanium-Oxygen Alloys," *Sci. Technol. Appl. Titanium*, Proc. Int. Conf., R.I. Jaffee, Ed., 745-763 (1970). (Equi Diagram; Experimental)
- 70Kor:** I.I. Kornilov, V.V. Vavilova, L.E. Fykin, R.P. Ozerov, S.P. Solowiev, and V.P. Smirnov, "Neutron Diffraction Investigation of Ordered Structures in the Titanium-Oxygen System," *Metall. Trans.*, 1, 2569-2571 (1970). (Equi Diagram; Experimental)
- 70Mar:** M. Marezio, P.D. Dernier, D.B. McWhan, and J.P. Reameka, "X-Ray Diffraction Studies of the Metal Insulator Transitions in Ti_4O_7 , V_4O_7 , and VO_2 ," *Mater. Res. Bull.*, 5, 1015-1024 (1970). (Equi Diagram, Crys Structure; Experimental)
- 70Mul:** L.N. Mulay and W.J. Danley, "Cooperative Magnetic Transitions in the Titanium-Oxygen System: A New Approach," *J. Appl. Phys.*, 41(3), 877-879 (1970). (Equi Diagram; Experimental)
- 70Sim1:** G.W. Simmons and E.J. Scheibner, "Order-Disorder Phenomena at the Surface of Alpha-Titanium-Oxygen Solid Solutions," *J. Mater.*, 933-949 (1970). (Equi Diagram; Experimental)
- 70Sim2:** P.Y. Simons and F. Dacheille, "Possible Topotaxy in the TiO_2 System," *Am. Min.*, 55, 403-415 (1970). (Meta Phases, Experimental)
- *70Yam:** S. Yamaguchi, K. Hiraga, and M. Hirabayashi, "Interstitial Order-Disorder Transformation in the Ti-O Solid Solution. IV. A Neutron Diffraction Study," *J. Phys. Soc. Jpn.*, 28(4), 1014-1023 (1970). (Equi Diagram; Experimental)
- 71Asb:** G. Asbrink, S. Asbrink, A. Magneli, H. Okinaka, K. Kosuge, and S. Kachi, "A Ti_3O_5 Modification of V_3O_5 -Type Structure," *Acta Chem. Scand.*, 25(10), 3889-3890 (1971). (Equi Diagram, Crys Structure; Experimental)
- 71Bur1:** L.A. Bursill and B.G. Hyde, "Crystal Structures in the {132} CS Family of Higher Titanium Oxides Ti_nO_{2n-1} ," *Acta Crystallogr. B*, 27, 210-215 (1971). (Crys Structure; Experimental)
- 71Bur2:** L.A. Bursill, B.G. Hyde, and D.K. Philip, "New Crystallographic Shear Families Derived from the Rutile Structure, and the Possibility of Continuous Ordered Solid Solution," *Philos. Mag.*, 23, 1501-1513 (1971). (Crys Structure; Experimental)
- 71Dub1:** A. Dubertret, "The Solid Solutions Alpha-Titanium-Oxygen and Alpha-Zirconium-Oxygen, Part I," *Métaux-Corros.-Ind.*, 46(545), 1-24 (1971) in French. (Crys Structure; Experimental)
- 71Dub2:** A. Dubertret, "The Solid Solution Alpha-Titanium-Oxygen and Alpha-Zirconium-Oxygen, Part II," *Métaux-Corros.-Ind.*, 46(546), 69-83 (1971) in French. (Crys Structure; Experimental)
- 71Dub3:** A. Dubertret and P. Lehr, "Zirconium-Oxygen and Titanium-Oxygen Solid Solutions," *Metallved., Mater. Simp.*, N.V. Ageev, Ed., 381-388 (1971) in Russian. (Crys Structure; Experimental)
- 71Ham:** P.J. Hampson and P.W. Gilles, "High-Temperature Vaporization and Thermodynamics of the Titanium Oxides. VII. Mass Spectrometry and Dissociation Energies of $TiO(g)$ and $TiO_2(g)$," *J. Chem. Phys.*, 55(8), 3712-3728 (1971). (Thermo; Experimental)
- 71Mar:** M. Marezio and P.D. Dernier, "The Crystal Structure of Ti_4O_7 , A Member of the Homologous Series Ti_nO_{2n-1} ," *J. Solid State Chem.*, 3, 340-348 (1971). (Crys Structure; Experimental)
- 71Nic:** M. Nicol and M.Y. Fong, "Raman Spectrum and Polymorphism of Titanium Dioxide at High Pressures," *J. Chem. Phys.*, 54(7), 3167-3170 (1971).
- 71Rao:** C.N.R. Rao, S. Ramdas, R.E. Loehman, and J.M. Honig, "Semiconductor-Metal Transition in Ti_3O_5 ," *J. Solid State Chem.*, 3, 83-88 (1971). (Equi Diagram, Crys Structure; Experimental)
- 71Stu:** D. Stull and H. Prophet, "JANAF Thermochemical Tables," NBS STP No. 37, Washington, D.C. (1971). (Thermo; Experimental)
- 72Dan:** W.J. Danley and L.N. Mulay, "Magnetic Studies on the Ti-O System: Experimental Aspects and Magnetic Parameters," *Mater. Res. Bull.*, 7, 739-748 (1972). (Equi Diagram; Experimental)
- 72Hul:** J.K. Hulm, C.K. Jones, R.A. Hein, and J.W. Gibson, "Superconductivity in the TiO and NbO Systems," *J. Low Temp. Phys.*, 7(3/4), 291-307 (1972). (Crys Structure; Experimental)
- 72Por:** V.N. Porter, W.B. White, and R. Roy, "Optical Spectra of the Intermediate Oxides of Titanium, Vanadium, Molybdenum, and Tungsten," *J. Solid State Chem.*, 4, 250-254 (1972). (Equi Diagram; Experimental)
- 72Roy:** R. Roy and W.B. White, "Growth of Titanium Oxide Crystals of Controlled Stoichiometry and Order," *J. Cryst. Growth*, 13/14, 78-83 (1972). (Equi Diagram; Experimental)
- 72Suz:** K. Suzuki and K. Sambongi, "High-Temperature Thermodynamic Properties in Ti-O System," *Tetsu-to-Hagane*, (*J. Iron Steel Inst. Jpn.*), 58(12), 1579-1593 (1972) in Japanese. (Equi Diagram; Experimental)
- 73Bar:** H.L. Barros, G.V. Chandrashekhar, T.C. Chi, J.M. Honig, and R.J. Sladek, "Specific Heat of Single-Crystal Undoped and V-Doped Ti_2O_3 ," *Phys. Rev. B, Condens. Matter*, 7(12), 5147-

- 5152 (1973). (Equi Diagram; Experimental)
- 73Gar:** E.A. Garcia, J. Com-Nougue, X. Lucas, G. Beranger, and P. Lacombe, "Variation of the Lattice Parameter of the Interstitial Ti-O Solid Solution as a Function of Oxygen Concentration," *C.R. Hebd. Seances Acad. Sci.*, **277**, 1291-1293 (1973) in French. (Crys Structure; Experimental)
- 73Kor:** I.I. Kornilov, "Relation of an Anomaly of Titanium Oxidation to a New Phase Diagram of the Titanium-Oxygen System with Suboxides," *Dokl. Akad. Nauk SSSR*, **208**(1-3), 356-359 (1973) in Russian. (Equi Diagram; Experimental)
- 73Mar:** M. Marezio, D.B. McWhan, P.D. Dernier, and J.P. Reameika, "Structural Aspects of the Metal-Insulator Transitions in Ti_4O_7 ," *J. Solid State Chem.*, **6**, 213-221 (1973). (Crys Structure; Experimental)
- 73Mer:** R.R. Merritt, B.G. Hyde, L.A. Bursill, and D.K. Philp, "The Thermodynamics of the Titanium-Oxygen System: An Isothermal Gravimetric Study of the Composition Range Ti_3O_5 to TiO_2 at 1304 K," *Philos. Mag.*, **274**, 628-661 (1973). (Equi Diagram, Thermo; Experimental)
- 73Rez:** V.A. Reznichenko and F.V. Khalimov, "Determination of a Variation in Free Energy in the Titanium Oxygen System Using an emf Method," *Protsesty Proizvod. Titana Ego Dvuokisi*, N.V. Ageev, Ed., 193-197 (1973) in Russian. (Thermo; Experimental)
- 73Sly:** N.P. Slyusar, A.D. Krivorotenko, E.N. Fomichev, A.A. Kalashnik, and V.P. Bondarenko, "Experimental Investigation of the Enthalpy of Titanium Oxide in the Temperature Range 500-2000 Degree K," *Teplofiz. Vys. Temp.*, **11**(1), 213-215 (1973) in Russian; TR: *High Temp.*, **11**(1), 190-192 (1973). (Equi Diagram; Experimental)
- 74Cor:** M. Cormier and F. Claisse, "Beta-Alpha Phase Transformation in Ti and Ti-O Alloys," *J. Less-Common Met.*, **34**, 181-189 (1974). (Meta Phases; Experimental)
- 74Gre:** I.E. Grey, C. Li, and A.F. Reid, "A Thermodynamic Study of Iron in Reduced Rutile," *J. Solid State Chem.*, **11**, 120-127 (1974). (Thermo; Theory)
- 74Rob:** W.R. Robinson, "The Crystal Structures of Ti_2O_3 , a Semiconductor, and $(Ti_{0.960}V_{0.100})_2O_3$, a Semimetal," *J. Solid State Chem.*, **9**, 255-260 (1974). (Crys Structure; Experimental)
- 75Cha:** M.W. Chase, J.L. Curnutt, H. Prophet, and R.A. McDonald, "JANAF Thermochemical Tables Supplement," *J. Phys. Chem. Data*, **(4)** (1975). (Thermo; Experimental)
- 75Pic:** C. Picard and P. Gerdanian, "Thermodynamics Study of Oxides TiO_{2-x} at 1050 °C," *J. Solid State Chem.*, **14**, 66-77 (1975) in German. (Thermo; Experimental)
- 76Bou:** G. Boureau and P. Gerdanian, "Thermodynamic Study of Interstitial Solid Solutions of Oxygen in Titanium at 1050 °C," *Acta Metall.*, **24**, 717-723 (1976). (Thermo; Experimental)
- 77Bau:** J.F. Baumard, D. Panis, and M. Anthony, "A Study of Ti-O System Between Ti_3O_5 and TiO_2 at High Temperature by Means of Electrical Resistivity," *J. Solid State Chem.*, **20**, 43-51 (1977). (Thermo; Experimental)
- 77Dec:** M. Dechamps, A. Quivy, G. Baur, and P. Lehr, "Influence of the Distribution of the Interstitial Oxygen Atoms on the Lattice Parameters in Dilute cph Titanium-Oxygen Solid Solutions (90-4000 ppm at)," *Scr. Metall.*, **11**, 941-945 (1977). (Crys Structure; Experimental)
- 78Koz:** A. Kozłowska-Rog and G. Rog, "Study on Phase Equilibria in the Titanium-Oxygen System within the Composition Range $TiO_{1.960}$ - TiO_2 by the Solid Galvanic Cell Technique," *Pol. J. Chem.*, **52**, 607-611 (1978). (Equi Diagram, Thermo; Experimental)
- 78Liu:** L.G. Liu, "A Fluorite Isotype of SnO_2 and A New Modification of TiO_2 ; Implications for the Earth's Lower Mantle," *Science*, **199**, 422-424 (1978). (Meta Phases; Experimental)
- 78Tet:** R. Tetot, C. Picard, G. Boureau, and P. Gerdanian, "High Temperature Thermodynamics of the Titanium-Oxygen System for O/Ti 1," *J. Chem. Phys.*, **69**(1), 326-331 (1978). (Thermo; Experimental)
- 79Dav:** D. David, E.A. Garcia, X. Lucas, and G. Beranger, "Study of the Diffusion of Oxygen in Alpha-Titanium, Oxidized Between 700 and 950 °C," *J. Less-Common Met.*, **65**, 51-69 (1979). (Equi Diagram; Experimental)
- 79Mit:** T. Mitsuhashi and O.J. Kleppa, "Transformation Enthalpies of the TiO_2 Polymorphs," *J. Am. Chem. Soc.*, **62**, (7-8), 356-357 (1979). (Equi Diagram, Thermo; Experimental)
- 79Ohs:** T. Ohsaka, S. Yamaoka, and O. Shimomura, "Effect of Hydrostatic Pressure on the Raman Spectrum of Anatase (TiO_2)," *Solid State Commun.*, **30**, 345-347 (1979). (Meta Phases; Experimental)
- 80Mam:** J.F. Mammone, S.K. Sharma, and M. Nicol, "Raman Study of Rutile (TiO_2) at High Pressures," *Solid State Commun.*, **34**, 799-802 (1980). (Meta Phases; Experimental)
- 81Mam:** J.F. Mammone, M. Nicole, and S.K. Sharma, "Raman Spectra of TiO_2 -II, TiO_2 -III, SnO_2 , and GeO_2 at High Pressure," *J. Phys. Chem. Solids*, **42**, 379-384 (1981). (Meta Phases; Experimental)
- 81Tet:** R. Tetot, C. Picard, and P. Gerdanian, "Direct Measurements of Delta $H(O_2)$ at 1323 K for Nonstoichiometric TiO ," *J. Chem. Phys.*, **75**(3), 1365-1367 (1981). (Thermo; Experimental)
- 82Gra:** B. Granier and P.W. Gilles, "High-Temperature Vaporization and Thermodynamics of the Titanium Oxides: XVII. Approximate Oxygen Potentials in Metal-Rich Solutions," *High Temp.-High Pressures*, **14**, 383-386 (1982). (Thermo; Experimental)
- 82Lep1:** Y. Le Page and P. Strobel, "Structural Chemistry of the Magneli Phases Ti_nO_{2n-1} ($4 \leq n \leq 9$). I. Cell and Structure Comparisons," *J. Solid State Chem.*, **43**, 314-319 (1982). (Crys Structure; Experimental)
- 82Lep2:** Y. Le Page and P. Strobel, "Structural Chemistry of the Magneli Phases Ti_nO_{2n-1} ($4 \leq n \leq 9$). II. Refinements and Structural Discussion," *J. Solid State Chem.*, **44**, 273-281 (1982). (Crys Structure; Experimental)
- 83Zad:** S. Zador and C.B. Alcock, "A Thermodynamic Study of Magneli and Point Defect Phases in the Ti-O System," *High Temp. Sci.*, **16**, 187-207 (1983). (Thermo; Experimental)
- 84Lep:** Y. Le Page and M. Marezio, "Structural Chemistry of Magneli Phases Ti_nO_{2n-1} ($4 \leq n \leq 9$). IV. Superstructure in Ti_4O_7 at 140 K," *J. Solid State Chem.*, **53**, 13-21 (1984). (Crys Structure; Experimental)

*Indicates key paper.

Ti-O evaluation contributed by J.L. Murray, Center for Materials Science, National Bureau of Standards, and H.A. Wriedt, 148 Washington Street, Pittsburgh, PA 15218. Work was supported by ASM International, the Office of Naval Research, and the National Bureau of Standards through the Metallurgy Division and the Office of Standard Reference Data. Literature searched through 1984. Dr. Murray is the ASM/NBS Data Program Category Editor for binary titanium alloys and Dr. Wriedt is the ASM/NBS Data Program Category Editor for binary oxygen alloys.